The Pennsylvania State University

The Graduate School

Intercollege Graduate Degree Program in Materials Science and Engineering

CATALYTIC ASPECTS OF NON-NOBLE METALS ON HYDROGEN GENERATION FROM HYDROLYSIS OF SODIUM BOROHYDRIDE

A Thesis in

Materials Science and Engineering

by

SUNYOUNG PARK

Submitted in Partial Fulfillment
of the Requirements
for the Degree of

Master of Science

August 2008

The thesis of Sunyoung Park was reviewed and approved* by the following:

Mirna Urquidi-Macdonald
Professor of Engineering Science and Mechanics
Thesis Co-Advisor

Melik C. Demirel
Title(s) Assistant Professor of Engineering Science and Mechanics
Pearce Development Professor
Thesis Co-Advisor

Digby D. Macdoald
Distinguished Professor of Materials Science and Engineering
Director, Center for Electrochemical Science and Technology

Joan M. Redwing
Professor of Materials Science and Engineering
Chair of Intercollege Graduate Degree Program in Materials Science and Engineering

*Signatures are on file in the Graduate School

ABSTRACT

In the generation of hydrogen from chemical hydrides, the catalyst is a key component. The use of expensive metals as catalysts limits the feasibility of the technology. Therefore, development of inexpensive and effective catalysts is very important in this field of study. In this work, cobalt based and aluminum alloy based catalysts for hydrogen generation from hydrolysis of alkaline stabilized sodium borohydride solutions were studied.

For the cobalt catalyst study, nanoporous cobalt thin films were fabricated by metallization of nanostructured poly(chloro-*p*-xylylene). The hydrogen generation performance of the cobalt PPX-Cl nano thin films (NTFs) was evaluated. Due to the high porosity of the nanostructure of the films, excellent hydrogen generation rates, which are comparable with novel metals, were achieved.

Cobalt powder (1.6μm dia.) was tested as a catalyst. It was postulated that passive film and re-precipitated film were formed on the cobalt catalyst in alkaline stabilized sodium borohydride solutions. To study the effect of the oxide films on the catalytic activity of the cobalt, ethylenediaminetetra acid (EDTA) was added to the electrolyte and hydrogen generation rates were measured. It was expected that EDTA would effectively suppress the cobalt oxide formation, increasing the hydrogen generation rate. However, the results showed that the hydrogen generation was decreased in the solutions with EDTA. In deaerated solutions, the hydrogen generation rates were increased regardless of the addition of EDTA. These results are explained as a blockage of Co-EDTA chelate, which decreases the absorption of species.

Evaluation of an aluminum alloy as a catalyst was carried out as a catalyst for sodium borohydride hydrolysis. The effects of EDTA and deaeration were also investigated. The results were opposite to that of cobalt. EDTA effectively increased the hydrogen generation rates, while deaeration had no effect on the hydrogen generation rates. Hydrogen was generated by both hydrolysis of $NaBH_4$ and the dissolution of aluminum in alkaline solutions.

TABLE OF CONTENTS

LIST OF FIGURES vii

LIST OF TABLES x

ACKNOWLEDGEMENTS xi

Chapter 1 INTRODUCTION 1

1.1 Hydrogen storage technologies 1
1.2 Sodium borohydride 3
1.3 Literature review 6
1.4 Problem statement 9
1.5 Objectives 9
1.6 Thesis outline 10

Chapter 2 COBALT CATALYST DEPOSITED ON NANOSTRUCTURED POLY(*P*-XYLYLENE) 11

2.1 Introduction 11
2.2 Experimental 13
2.3 Results 18
2.4 Conclusions 28

Chapter 3 STUDY OF COBALT AS INEXPENSIVE AND EFFECTIVE CATALYST FOR THE PRODUCTION OF HYDROGEN IN ALKALINE STABILIZED SODIUM BOROHYDRIDE SOLUTIONS 30

3.1 Introduction 30
3.2 Experimental Procedure 35
3.3 Results 38
3.4 Conclusions 40

Chapter 4 STUDY OF ALUMINUM ALLOY FOR THE PRODUCTION OF HYDROGEN FROM ALKALINE STABILIZED SODIUM BOROHYDRIDE SOLUTIONS 42

4.1 Introduction 42
4.2 Experimental 45
4.3 Results 47
4.4 Conclusions 55

Chapter 5 RECOMMENDATIONS 57

Bibliography 61

Appendix A Achievement 64

LIST OF FIGURES

Figure **1-1**: Decomposition rate of sodium borohydride as a function of temperature and pH [4]. 5

Figure **2-1**: Schematic of oblique angle vapor deposition of poly(*p*-xylylene) (PPX) films. Vaporized chloro-*p*-xylene monomers are directed to the substrate then polymerized. (α : flux angle to the substrate, β : angle of polymer growth on the substrate) [21]..... 12

Figure **2-2**: Schematic of nanostructured poly(p-xylylene) film. The diameter of polymer strand are ~150nm [18]. 12

Figure **2-3**: Schematic of polymerization of poly(chloro-*p*-xylylene) (PPX-Cl) [20]..... 14

Figure **2-4**: Schematic of hydrogen generation measurement set up. Hydrogen released from the solution replaces water in burrets. The volume of hydrogen gas measured recorded every five minutes. The temperature of reaction vessels were kept constant at 20°C. 17

Figure **2-5**: Cross sectional SEM images of PPX films by (a) oblique angle and (b) conventional method (scale bar : 20 μm) [22]. 18

Figure **2-6**: SEM images for (a) 15 min cobalt bath time on nanostructured PPX-Cl (both microscopic and macroscopic porosity are observed), (b) 100min cobalt bath time on nanostructured PPX-Cl (less porous compared to (c)) are shown. (c) Metallized planar PPX-Cl film which shows isolated patches of cobalt (scale bar: 50μm), and (d) metallized nanostructured PPX-Cl at a 120-min bath time, which shows delaminating of the cobalt film (scale bar: 200μm) [22]. 21

Figure **2-7**: AFM images for (a) 15 min and (b) 60 min cobalt bath times are shown. The scale bars for the AFM scans: *X*, 0.5μm/div; *Y*, 0.5μm/div; *Z*, 100nm/div. (c) Cobalt weight percentage on nanostructured PPX film obtained from the EDAX data with respect to the cobalt bath time. (d) Roughness of nanoporous cobalt film on nanostructured PPX-Cl with varying bath times [22]. 22

Figure **2-8**: EDAX spectra of Co-PPX 60 min cobalt bath time sample. 23

Figure **2-9**: Hydrogen generation by the nano structured Co catalyst (1% NaOH, 2.5% $NaBH_4$, 20°C).....23

Figure **2-10**: (a) The hydrogen release rate (ml/(min*cm^2)) from the nanoporous and planar cobalt surface measured in 2.5% NaBH4 and 1% NaOH at 25 °C. (b) Hydrogen release rate dependence on NaBH4 concentration measured for a 100-min bath time sample at a pH of 11.5 and at 25 °C. (c) Hydrogen release rate dependence on pH measured for a 100-min bath time sample with 2.5% NaBH4 concentration at 25 °C [22].....27

Figure **3-1**: Pourbaix diagram of cobalt in water at 25°C [30]. 31

Figure **3-2**: Cobalt PPX film in deaerated alkaline solutions (pH = 12.885, T = 20°C). The color change of cobalt PPX-Cl film indicates the formation of oxide films on the surface of catalyst. (a) : initial state and (b) : 93 hours later. 33

Figure **3-3**: Structure of EDTA (a) and Metal-EDTA chelate (b). 34

Figure **3-4**: Proposed schematic of passive films on cobalt in alkaline solutions. It is assumed that Co-EDTA chelate prevent the formation of outer oxide layer in the presence of EDTA. The formation of CoOOH, Co_3O_4 may depend on the potential of sample.....35

Figure **3-5**: Experimental setup for open circuit potential measurement.....37

Figure **3-6**: Pictures of cobalt rod surface before (a) and after (b) 1 hour open circuit potential measurement in 0.261M NaOH solution.....38

Figure **3-7**: Influence of 0.01M EDTA on hydrogen release of naturally aerated and deaerated 2.5% $NaBH_4$ solutions with 1% NaOH. 40

Figure **4-1**: Pourbaix diagram of aluminum-water system at 25°C [30]. 44

Figure **4-2**: Aluminum alloy examined as a catalyst for hydrolysis of sodium borohydride. The sample was hold in epoxy resin for sample preparation. 47

Figure **4-3**: Energy dispersive x-ray result showing composition of aluminum alloy 48

Figure **4-4**: The effects of NaOH concentration and deaeration on hydrogen generation of Al alloy. 1, 5, 10, 15 % NaOH, 2.5% $NaBH_4$ solutions with naturally aerated and deaerated (N_2) solutions were used at 19~23°C. 50

Figure **4-5**: The effects of NaOH concentration (1, 5, 10 and 15 wt.%) and deaeration of solutions at 19~23°C. Each solutions contains 2.5 wt% $NaBH_4$. ... 51

Figure **4-6**: Hydrogen generation rate of Al alloy sample in 0.261M NaOH, 0.677 M $NaBH_4$ solutions at 20°C. 52

Figure **4-7**: Hydrogen generation from aluminum in 0.26M NaOH solutions at 20°C. 54

Figure **4-8**: Aluminum alloy catalyst before (a) and after (b) one hour hydrogen generation experiment in alkaline (pH=13) stabilized 2.5% $NaBH_4$ solution. (T = 20°C) 54

LIST OF TABLES

Table **2-1**: Hydrogen generation rate of catalysts from alkaline stabilized $NaBH_4$ solutions in various conditions [22].....28

Table **4-1**: EDAX ZAF quantification (standardless) of Al alloy.....48

ACKNOWLEDGEMENTS

I would like to appreciate Dr. Mirna Macdonald for her insightful advices and discussions as academic advisor. Her efforts and generosity towards me made this work possible. She made every effort to encourage me and take care of my future.

I would like to extend my appreciation to Dr. Melik Demirel as a co-advisor. He gratefully accepted me in his group and let me work in his lab. I could see more insights while I was working on one of his projects.

And also, thanks to the committee members for this thesis, including Dr. Digby Macdonald, who should be recognized for their help.

For lab experiments, Omar Camacho helped me set up experiments and advised me with his insightful knowledge. In Dr. Demirel's group Niranjan Malvadkar and Dr. Hui Wang were dedicated in this study by fabrication of Co-PPX films. I appreciate them all.

I would express my gratitude to the Republic of Korea Army for giving me this opportunity and financial support to complete Master's degree for two years.

And finally, I would like to thank my wife Sunghee for her dedication and support during my study at Penn State and my daughter Grace for her love.

Chapter 1

INTRODUCTION

We are living on the planet Earth, which has limited resources. And we are consuming incredible energy each day. The soaring price for oil today proves the facts. The growth of the energy demand has accelerated new kinds of energy sources.

One of the candidates from various natural, clean energy sources is hydrogen. The hydrogen economy is at hand. The researchers are working on fuel cells. Governments and companies invest huge amounts of money on research. Hydrogen attracts our attention for many reasons. It is clean and environmentally friendly. The only byproducts by of the fuel cell are water and heat. The energy density of hydrogen is higher than the fossil fuels.

1.1 Hydrogen storage technologies

A review of current hydrogen storage technologies is important, before we take a careful look at sodium borohydride. Brief descriptions of each technology are presented including advantages and disadvantages.

1. Hydrogen gas tank

Compressed hydrogen gas is stored in high-pressure tanks of 5,000 ~ 10,000 psi (pound per square inch). The high pressure of hydrogen gas tanks is due to the low energy density of hydrogen, which is 0.08988g/L (0°C, 101.325kPa). The compressed hydrogen gas technology does not require additional devices, for example, reformers, catalysts or coolants. However, there are safety issues to be considered due to the high pressure of the tank.

2. Liquefied hydrogen

The disadvantage of compressed gas is the need for large volume tanks. Liquefaction of hydrogen gas can solve that problem. The energy density of liquid hydrogen is higher than compressed hydrogen. Volumetric capacity of liquefied hydrogen is 0.07 kg per liter, while that of compressed hydrogen in a 10,000 psi compressed tank is 0.03kg per liter. However, first we need to liquefy hydrogen. Moreover, liquefying requires insulation, which means the reduction of volumetric and gravimetric capacities.

3. Metal hydrides

In a metal hydride storage system, the hydrogen atoms are absorbed into crystal interstitials of metal forming metal hydride. This reaction of metal hydride formation is a reversible process. When hydrides form, the heat is released. In the dehydriding process, heat is required. Metal hydride is much safer than compressed hydrogen gas. Moreover, the volumetric density is about 0.06 kg per liter, which is comparable to the liquefied

hydrogen. However, due to the heavy weight of metal compounds, the gravimetric density of metal hydrides is low, which is 5.5 wt.%. More issues with metal hydrides are heat management and slow kinetics.

4. Chemical hydride

Chemical hydrides release hydrogen gas when they are in contact with other substances – water, catalysts, and so on. Currently, the most investigated chemical hydrides are sodium borohydride ($NaBH_4$) and magnesium hydride (MgH_2). The hydrolysis reaction can be controlled by pH, the temperature of chemical hydride solutions and catalysts. The rate of hydrolysis reaction is high and the hydrogen content of chemical hydrides is also high. However, it is not easy to convert the dehydrogenated products into the original forms of chemical hydrides. For that reason, energy for recycling should be considered when discussing the efficiency of a chemical hydride hydrogen generation system. The regeneration of chemical hydrides and its cost are current issues and researches on them are being carried out.

1.2 Sodium borohydride

The necessity of hydrogen generation for the war brought on the development of chemical hydride [1]. Among many scientists, Herbert C. Brown, Nobel Prize winner, contributed to the development of sodium hydride in the 1940s and 1950s. Schlesinger et al. [2] reported that sodium borohydride is a highly stable crystalline chemical that can be

dissolved in ambient temperature water without violent reactions. However, it releases hydrogen in the presence of catalysts, acids, or in high temperature. Sodium borohydride solution reacts with the water producing hydrogen gas and the sodium borates.

$$NaBH_4 + 2H_2O \rightarrow NaBO_2 + 4H_2,\ \Delta H = -217kJ/mol \qquad (\mathbf{1.1})$$

The reaction rate is determined by the pH and temperature according to the report of Kreevoy and Jacobson [3].

$$\log t_{1/2} = pH - (0.034T - 1.92) \qquad (\mathbf{1.2})$$

where $t_{1/2}$ is the half-life of $NaBH_4$ solution in minutes at the certain pH and the absolute temperature.

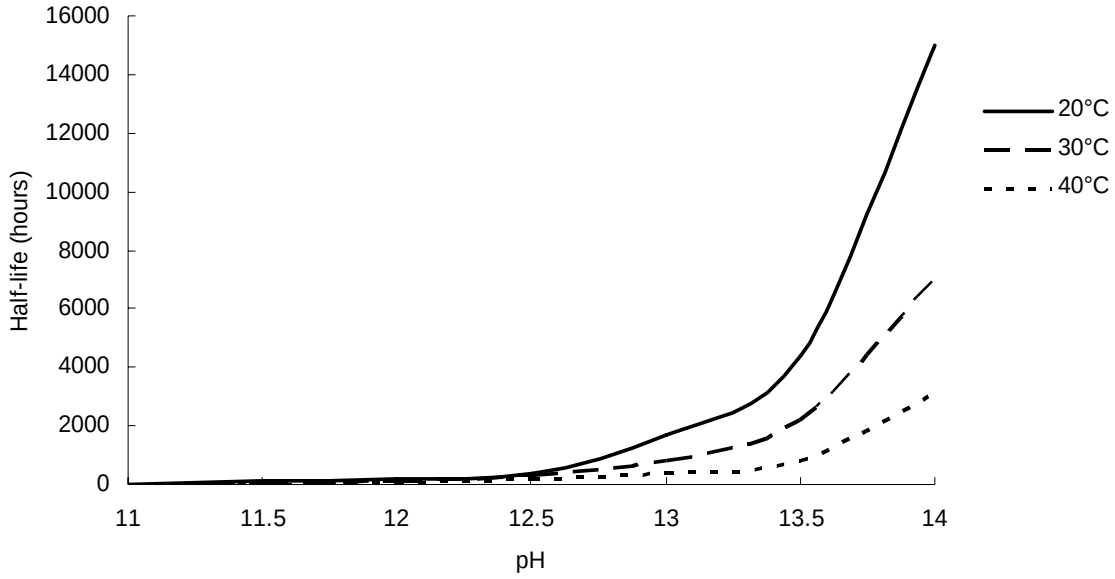

Figure **1-1**: Decomposition rate of sodium borohydride as a function of temperature and pH [4].

Sodium borohydride is a non-toxic, chemical compound containing four atoms of hydrogen. The recyclability of this chemical compound gives positive feasibility as a source of hydrogen. Sodium borohydride is also used as reducing agent in organic chemistry and as cooling media. The current cost of $NaBH_4$ is about US$55 per kg, which is considered a disadvantage [1]. Considering four moles of hydrogen by the reaction from the equation 1.1, the cost of hydrogen from $NaBH_4$ is approximately $260 per kg. This is not a promising source of hydrogen considering its current price. However, we can expect a price cut from the mass production and recycling of sodium metaborate to sodium borohydride [5, 6].

1.3 Literature review

A great deal of research has been conducted to achieve a high hydrogen generation rate by developing new catalysts and systems. From the research, I have focused on catalysts for hydrolysis of $NaBH_4$.

Patel et al. [7] reported Pd/C thin films by pulsed laser deposition (PLD) for hydrolysis of $NaBH_4$. They claimed that the disordered structure and irregular morphology of carbon supported by PLD provide a high surface area for Pd film. Various conditions of vacuum, 20, 30, 50 and 65 Pa of pressure were used on the deposition of carbon followed by Pd deposition. 0.025±0.001M of $NaBH_4$ was used with 0.1M of NaOH for stabilization. The reserchers compared the hydrogen production rate of Pd/C films by PDL with Pd/C powder and showed a higher hydrogen production rate of the films. Unfortunately, they did not show any comparison with other catalysts developed by other researchers.

Krishnan et al.[8] reported catalytic activity of PtRu supported on various materials. They claimed that cobalt boride (CoB) formation on Co_3O_4 and $LiCoO_2$ reduced by $NaBH_4$ contributed high activities of these metal oxides. However, they did not explain why the hydrogen generation rate decreased as a function of time.

Kim et al.[9] developed a filamentary Ni Co catalyst with sylene-butadiene-rubber as a binder. They reported a maximum hydrogen release rate of 96.3ml/min.g with 12.5wt. % $NaBH_4$ at pH 13 and at room temperature. They compared Co and a mixture of Co and filamentary Ni in terms of specific surface area and pore size distribution, and also reported an ideal content of filamentary Ni to Co of 20%. Finally, they reported that

a high purity of 99.9% hydrogen gas was generated. Although they could produce an inexpensive catalyst for this area, the performance of the catalyst was not enough for actual application. In their later work [10], they studied the degradation of filamentary Ni catalyst. They confirmed the formation of film consists of $Na_2B_4O_7 \cdot 10H_2O$, KB_xO_y and B_2O_3, accompanied by accumulation of K, Na, and B on the catalyst by characterization techniques. They concluded that the decrease of hydrogen generation rate to 70% after 200 cycles compared to the initial rate was due to the reduction of a specific surface area by the accumulation and formation of chemical compounds.

Wu et al. [11] reported cobalt boride catalysts with various temperature heat treatments. They observed phase changes of catalysts which are amorphous - a mixture of cobalt boride, cobalt metal, and pure metal cobalt. They claimed that these phase changes were dependent on the temperature of heat treatment. They reported a hydrogen release rate of 2970ml/min/g, with the CoB catalyst heat treated at 500 degrees Celsius. However, they did not mention the exact composition of the catalysts and degradation problem of their catalysts.

Kojima et al. [12] reported the catalytic activities of various metal and metal oxides and concluded that Pt-$LiCoO_3$ is the most effective among the catalysts.

Ru catalyst supported on ion exchange resin beads was reported by Amendola et al. [13]. They demonstrated the effects of $NaBH_4$, NaOH concentrations and temperature. They reported a ~8ml/sec.g (480ml/min.g) of hydrogen generation rate with 1 wt% of NaOH and ~12.5 wt% of $NaBH_4$. They claimed that the slow rate at the beginning with high concentrations of $NaBH_4$ was due to the high viscosity of the solution. They also

claimed that high concentrations of hydroxyl ions from the NaOH decreased water molecules available for hydrolysis reaction.

Lee et al. [14] reported a Co-B catalyst supported on Ni foam of 2mm thickness. A simple dipping method was introduced – dipping Ni support into $CoCl_2$ solution, followed by immersing it into the mixture of 20 wt% $NaBH_4$ and 1 wt% NaOH solution as a reducing agent. The effect of heat treatment in various temperatures was also tested, and they confirmed the changes of the structure from an initial amorphous state to a crystallized and decomposed state by x-ray diffraction result. They claimed that their Co-B supported on Ni foam exhibited 374ml/min.cm^2 of hydrogen release rate with the catalyst made by 20 dipping cycles. However, the results could not be compared with other ones due to the difference of units. They reported 45kJ/mol as activation energy for hydrolysis of $NaBH_4$ with this catalyst.

Cho et al. [15] reported Co and Co-P on a Cu substrate by an or the electrodeposititon method. They reported the activity of their catalyst as 954ml/min.g with the solution composed of 1 wt% of NaOH and 10 wt% of $NaBH_4$ at 30°C. The catalysts have different morphologies, depending on the deposition current density and the time of deposition that influenced the hydrogen generation rates. They concluded that with elecrodeposition, the Co-P catalyst showed a higher order of magnitude activity than Co catalyst.

Ingersoll et al. [16] reported the Ni-Co-B catalyst, which showed the hydrogen generation rate of 2608ml/min.g at 28°C. They claimed that their catalyst showed the highest catalytic activity at 15 wt% NaOH, which is unusual with non-noble metals. And

also, they claimed that the activity of a catalyst is independent of the concentration of $NaBH_4$.

1.4 Problem statement

The catalytic activities of novel metals such as platinum and ruthenium are known to be excellent for the hydrolysis of sodium borohydride. However, the amounts of metals mentioned above are limited; that is the reason they are called 'precious' metals. To promote the use of hydrogen as a source of energy in human life, the development of inexpensive and efficient catalysts for hydrogen generation is essential.

1.5 Objectives

The objectives of this thesis were to:

- Investigate inexpensive catalysts for hydrogen generation from alkaline stabilized sodium borohydride solutions.
- Test the catalytic activities of cobalt deposited on poly p-xylylene substrate, cobalt powder and aluminum alloy, which are more inexpensive and effective.
- Investigate hydrogen generation from aluminum in alkaline solutions with the combination of $NaBH_4$.

1.6 Thesis outline

In Chapter One, the background of hydrogen storage technologies and sodium borohydride is introduced. Also, catalysts developed for the hydrolysis of sodium borohydride from the literatures are summarized. Finally, problems of this field of study and objective of this thesis are stated.

In Chapter Two, cobalt deposited, nano-structured polymer thin film is introduced. The concept and preparation process are described and its catalytic activities in different conditions are reported.

Chapter Three focused mainly on the cobalt particle as a catalyst. Experiments on hydrogen generation in various conditions were conducted. And also, oxidation of cobalt particles was studied.

Chapter Four contributed to the aluminum alloy, examining its catalytic activity for the hydrolysis of sodium borohydride and its reaction with sodium hydroxide.

Finally, recommendations for future works, which could contribute to this area of research, are presented in Chapter Five.

Chapter 2

COBALT CATALYST DEPOSITED ON NANOSTRUCTURED POLY(*P*-XYLYLENE)

2.1 Introduction

The use of nanostructured materials in energy applications is widely accepted due to its unusual chemical and physical properties. As mentioned in Chapter One, extensive research has been conducted on the increasing surface area of catalysts by using substrates which have high surface areas, for example, carbon nanotubes [17] and metal foams [14].

Recently, nanostructured polymer thin films have been developed by oblique angle vapor deposition [18-20]. The nanostructured poly (chloro-*p*-xylylene) (PPX-Cl) films have about 37,500,000 columns on unit square millimeters. Figure 2-1 shows the chemical structure of PPX-Cl. The diameter of each column is about 50 ~ 200 nm as shown in Figure 2-2. The growth of polymer nanostructures by oblique angle vapor deposition is affected by geometrical self-shadowing [18], surface diffusion along the substrate of monomers and surface roughening and nucleation [19-21].

The metallization of nanostructured PPX has important use as materials in variety of applications, for example, catalysts, medical implants, coatings and so on. It is reported [18] that the nickel metallization of nanostructured PPX films has been developed by non-covalent binding of pyridine to PPX-Cl and covalent binding of

palladium colloid to pyridine as an initiation process. Palladium is used as a catalyst for electroless metallization and it is not exposed on the surface of metal-PPX films.

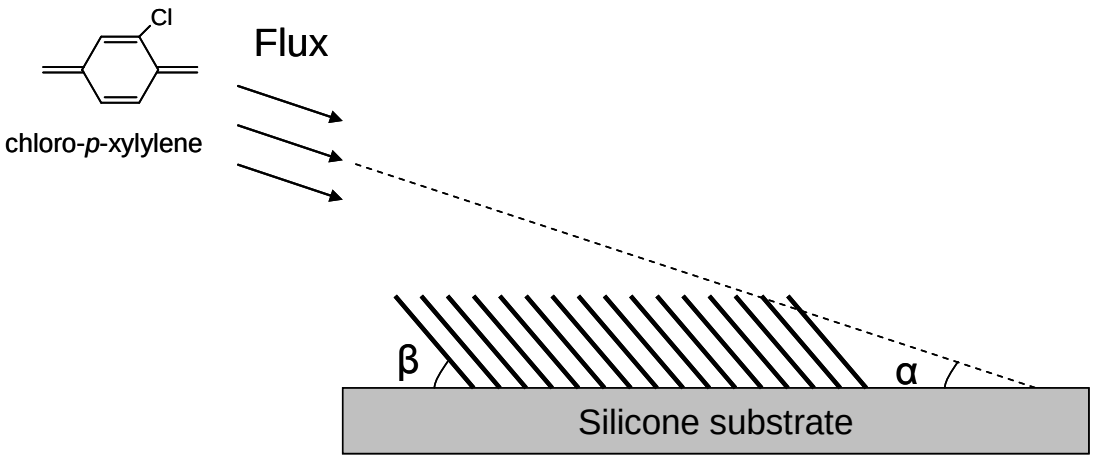

Figure **2-1**: Schematic of oblique angle vapor deposition of poly(*p*-xylylene) (PPX) films. Vaporized chloro-*p*-xylene monomers are directed to the substrate then polymerized. (α : flux angle to the substrate, β : angle of polymer growth on the substrate) [21]

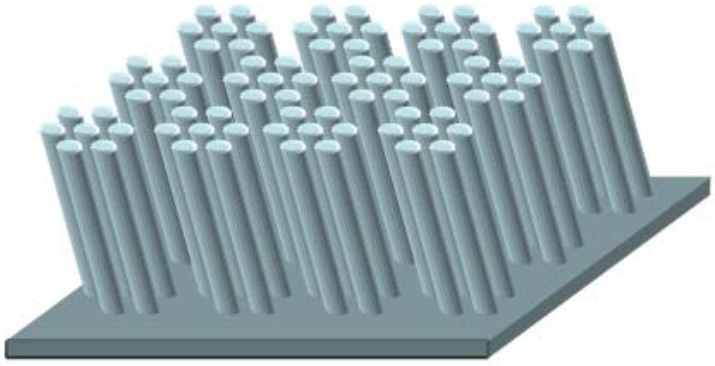

Figure **2-2**: Schematic of nanostructured poly(p-xylylene) film. The diameter of polymer strand are ~150nm [18].

By using the high porosity of nanostructured polymer films, which is fabricated by oblique angle deposition, an effective catalyst can be fabricated by metallization of PPX film. In addition, while the cost of fabricating nanostructured PPX films is inexpensive, the process is simple. Cobalt is widely used in catalyst research on the hydrolysis of sodium borohydride because of its good catalytic activity. Moreover, it is less expensive than noble metals, for example, platinum or ruthenium. This chapter is dedicated to the investigation of catalytic activity of cobalt deposited, nanostructured PPX films in alkaline stabilized $NaBH_4$ solutions. An important feature of PPX film is that it could provide the possibility of fabricating surfaces exhibiting tunable roughness [19-21]. Therefore, this is a good reason to choose the nanostructured PPX film as a substrate for catalyst.

2.2 Experimental

Materials

All chemicals used were A.C.S reagent grade and deionized water of 18.1 MΩ cm was used for all experiments. Dichloro-[2, 2] paracyclophane (DCPC) was purchased from Parylene Distribution Services and deposited on p-type Si (100) wafers purchased from Wafernet Inc (San Jose, CA).

Preparation of Nanostructured PPX-Cl film

Sonification of silicon wafers in acetone was carried out, followed by washing with deionized water and drying with nitrogen gas. The wafers were immersed in a

solution of 1:1 volume ratio of HCl and CH_3OH for 30 minutes. Next, the wafers were washed with deionized water and immersed in concentrated H_2SO_4 (95-98% wt.%) for 30 minutes, followed by deionized water washing and nitrogen gas drying. A self-assembled monolayer (SAM) solution of 1% (v/v) allyltrimethoxysilane in toluene, containing 0.1% (v/v) acetic acid, was used to enhance the adhesion of PPX film to the substrate. The silicone wafers were immersed in SAM solution for 60 minutes, then sonicated in anhydrous toluene for 10 minutes. The wafers were baked at 140 ºC for five minutes.

Nanostructured PPX films were deposited on the silicon substrate by oblique angle vapor deposition ($\alpha = 10^{o}$). Dimers of DCPC(0.3g) were placed in a vaporizer (175 ºC) at about 10 mTorr vacuum pressure. The temperature of pyrolysis was controlled at 690 ºC and the 50 μm thick nanostructured films were deposited. Figure **2-3** shows the schematic process of PPX film polymerization.

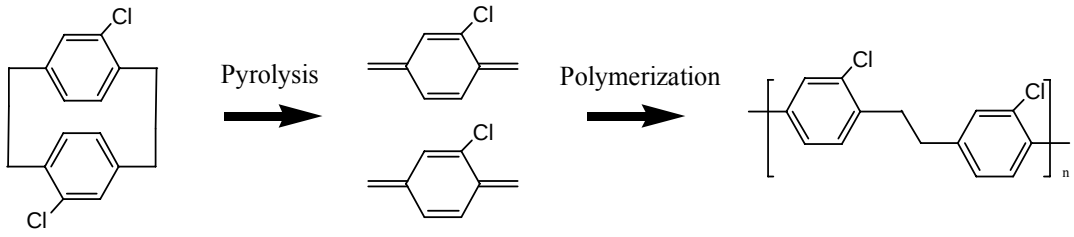

Figure **2-3**: Schematic of polymerization of poly(chloro-*p*-xylylene) (PPX-Cl) [20].

Metallization of PPX-Cl Films

The PPX nanostructured thin films (NTFs) were metallized by the following procedure of a 48 hours immersion of the films in 1M pyridine solution. The films were treated by DI water washing and nitrogen gas drying. The films were then immersed in a

Pd(II)-based colloidal solution for 45 minutes at room temperature. Pd was used for electroless metallization of nanostructured polymer films. The absence of Pd after the metallization process was proved through the characterization of the samples. The preparation of a Pd(II) based solution was carried out by Na_2PdCl_4 hydrolysis in a solution of 0.01M NaCl at pH 5. The film was then washed with DI water and dried by N_2 gas.

The metallization bath was prepared by following procedure. Chemicals of EDTA (0.9g), ammonium chloride (1g) and cobalt chloride (0.6g) were dissolved in 15ml DI water at pH 8.2. 0.4 g of Boranedimethylamine in 5ml DI water was prepared and mixed with the bath. The films were immersed in the bath at room temperature. Various deposition time samples of 15, 30, 45, 60, 120 and 240 minutes were prepared. The films were washed and dried after cobalt depositions.

Film Characterization

The surface topography images were collected by atomic force microscope (Veeco Metrology, CA) at room temperature, using triangular cantilever silicon nitride (SiN) contact mode tips. For cross sectional and surface characterization, a Philips XL-30 scanning electron microscope (SEM) was used. An energy dispersive x-ray (EDAX) was used to analyze the composition of cobalt films, which is shown in Figure 2-8.

Hydrogen release rate

Aqueous solutions of 2.5 % $NaBH_4$ (0.677 M) and 1 % NaOH (0.261 M) were used for all the experiments at room temperature. The pH (=13) was kept constant, while

the solution temperature was maintained at 25 ±0.5 ºC. The solution was contained in the 125 ml beaker, and the hydrogen gas generated was collected in the water column, which was immersed into a beaker. The amount of hydrogen released was recorded with respect to time. From these data, the release rate was obtained by differentiating the hydrogen release volume with respect to time. The hydrogen release rate was measured in ml of H_2 per square centimeter of the cobalt film per minute (ml/(min*cm^2). The rate was also measured in mass units as ml of H_2 per gram of cobalt per minute (ml/(min*$g_{catalyst}$)) by calculating the mass of cobalt deposited on the PPX-Cl film.

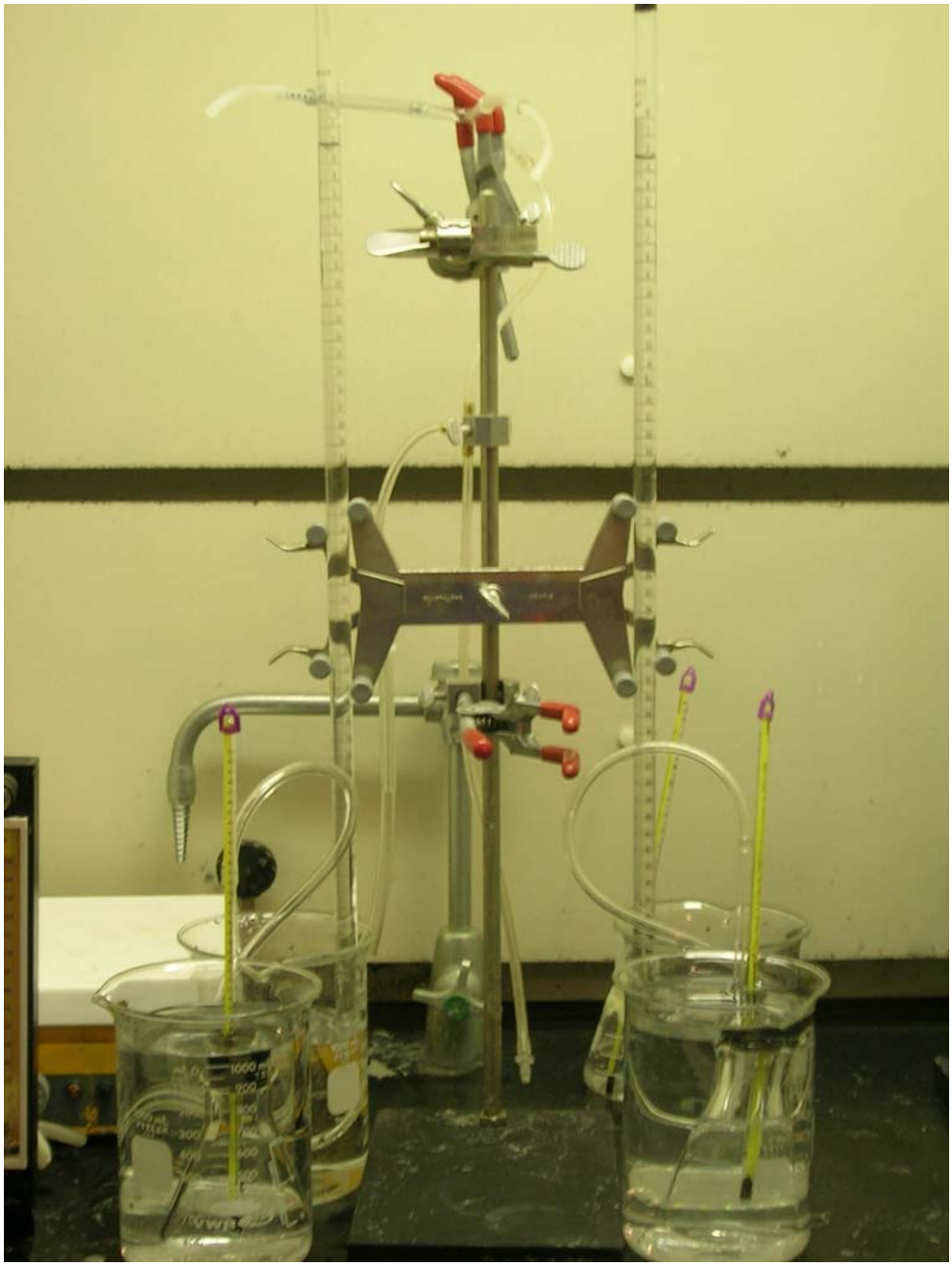

Figure **2-4**: Schematic of hydrogen generation measurement set up. Hydrogen released from the solution replaces water in burrets. The volume of hydrogen gas measured recorded every five minutes. The temperature of reaction vessels were kept constant at 20°C.

2.3 Results

Two types of PPX-Cl films which are nanostructured and planar were prepared by oblique angle vapor deposition. The cross sectional scanning electron microscopy (SEM) images in Figure 2-5 shows the difference in structures of columnar and planar PPX-Cl films. The nanoscale polymer columns were observed in PPX-Cl films by oblique angle vapor deposition while the planar films did not have nanostructure. Metallization of both nanostructured and planar PPX-Cl films were carried out.

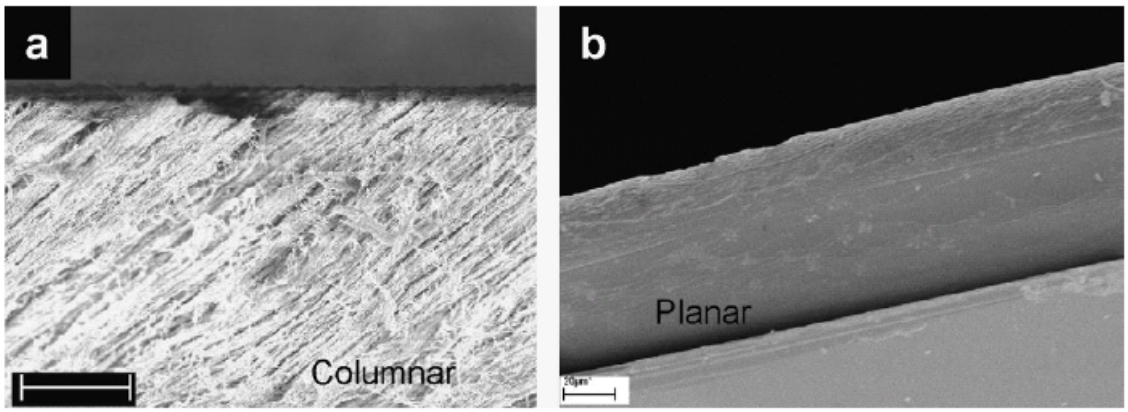

Figure **2-5**: Cross sectional SEM images of PPX films by (a) oblique angle and (b) conventional method (scale bar : 20 μm) [22].

The non-covalently bonded pyridine to the nanostructured PPX-Cl films provides sites for covalent Pd(II) binding for metallization of PPX-Cl films [18]. This simple electroless metallization process allows the control of cobalt morphology as well as topology on the nanostructured PPX-Cl film substrates. The conformal metallization of nanoporous cobalt films could be achieved as shown in the SEM images in Figure 2-6. Figure 2-6 (a) and (b) show the result of differentiating immersion of PPX-Cl films in the

cobalt bath. The 100 minute cobalt bath time sample in Figure 2-6 (b) is less porous than the 15 minute sample shown in Figure 2-6 (a). The higher bath time resulted in a decrease in porosity of the films. However, cobalt bath time of more than two hours resulted in cracks in the cobalt films due to the accumulated stress shown in Figure 2-6 (d). Adhesion of cobalt deposited nanostrutured PPX-Cl films were evaluated by Scotch tape® delamination test and the results showed delamination of less than 5%. The cobalt deposition on planar PPX-Cl films did not show satisfactory results. The SEM image of the cobalt planar films is shown in Figure 2-6 (c). The adsorption of pyridine on planar PPX-Cl films was not as good as that on nanostructured films. The patch of cobalt films formed on the surface which resulted in poor adhesion.

Figure 2-7 shows the atomic force microscope images of metallized PPX-Cl films. The images in Figure 2-7 (a) and (b) show the 15 minutes and 60 minutes cobalt bath immersed PPX-Cl films. The size difference of particles is also shown, with an average size of 250 nm in (a) and about 1 μm average size in (b) respectively. The amorphous cobalt films begin to grow at the tip of the columns in cobalt bath during metallization process.

The cobalt compositions of the films were characterized with EDAX. The composition data of each bath time samples are shown in Figure 2-7 (c). The weight percentages of cobalt on nanostructured PPX-Cl films were increased as the time of immersion in cobalt bath increased. Figure 2-7 (c) also indicates the maximum concentration of cobalt which is about 90 percent. The concentration data of cobalt are well matched to the SEM images of morphology in Figure 2-6 (a) and (b). Surface

roughness of the films was calculated from AFM images and is shown in Figure 2-7 (d). The roughness of cobalt shows an increasing trend as shown in the figure.

It is important to clarify that Pd used as a binding catalyst for Co metallization is not exposed to the surface of the films, because of possible catalytic reaction of Pd on the hydrolysis of $NaBH_4$. EDAX data for all different cobalt bath time samples proved that Pd is not exposed to the surface of the Co-PPX catalysts. Among the EDAX data, 60 minute cobalt bath time sample are shown in Figure 2-8. By the results in the Figure, it is reasonable to mention that Pd does not react in the hydrogen generation process.

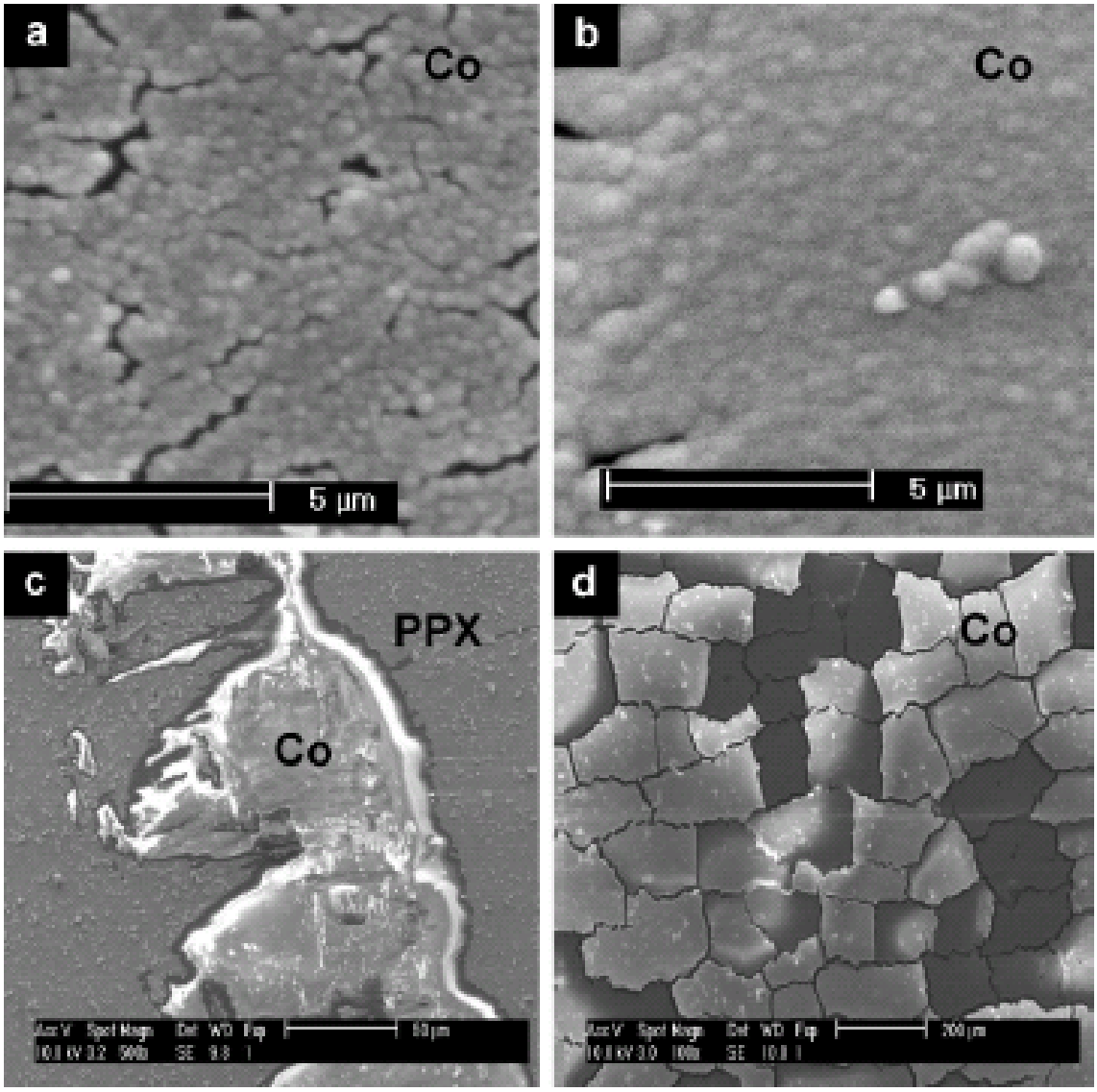

Figure **2-6**: SEM images for (a) 15 min cobalt bath time on nanostructured PPX-Cl (both microscopic and macroscopic porosity are observed), (b) 100min cobalt bath time on nanostructured PPX-Cl (less porous compared to (c)) are shown. (c) Metallized planar PPX-Cl film which shows isolated patches of cobalt (scale bar: 50µm), and (d) metallized nanostructured PPX-Cl at a 120-min bath time, which shows delaminating of the cobalt film (scale bar: 200µm) [22].

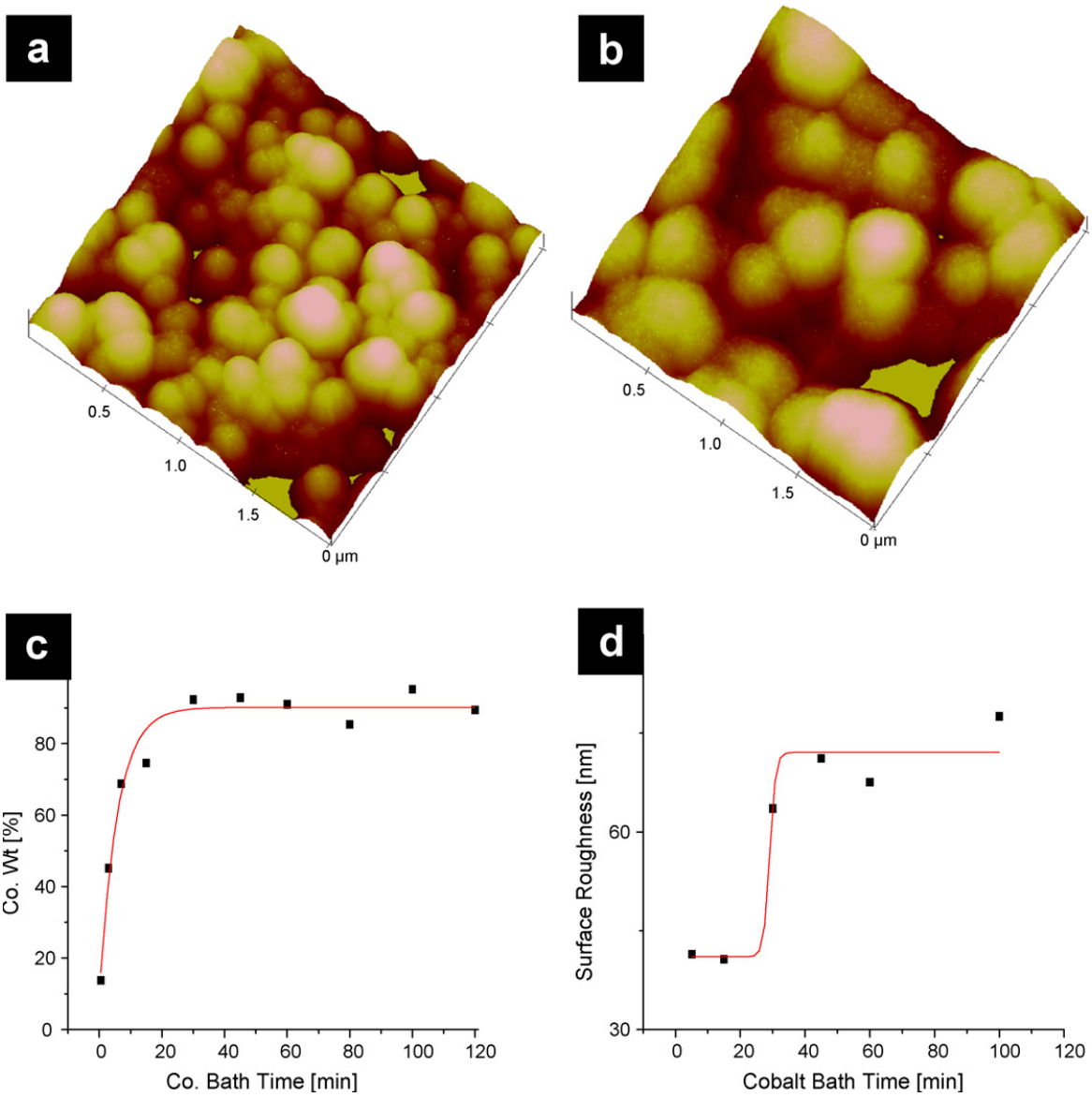

Figure **2-7**: AFM images for (a) 15 min and (b) 60 min cobalt bath times are shown. The scale bars for the AFM scans: *X*, 0.5µm/div; *Y*, 0.5µm/div; *Z*, 100nm/div. (c) Cobalt weight percentage on nanostructured PPX film obtained from the EDAX data with respect to the cobalt bath time. (d) Roughness of nanoporous cobalt film on nanostructured PPX-Cl with varying bath times [22].

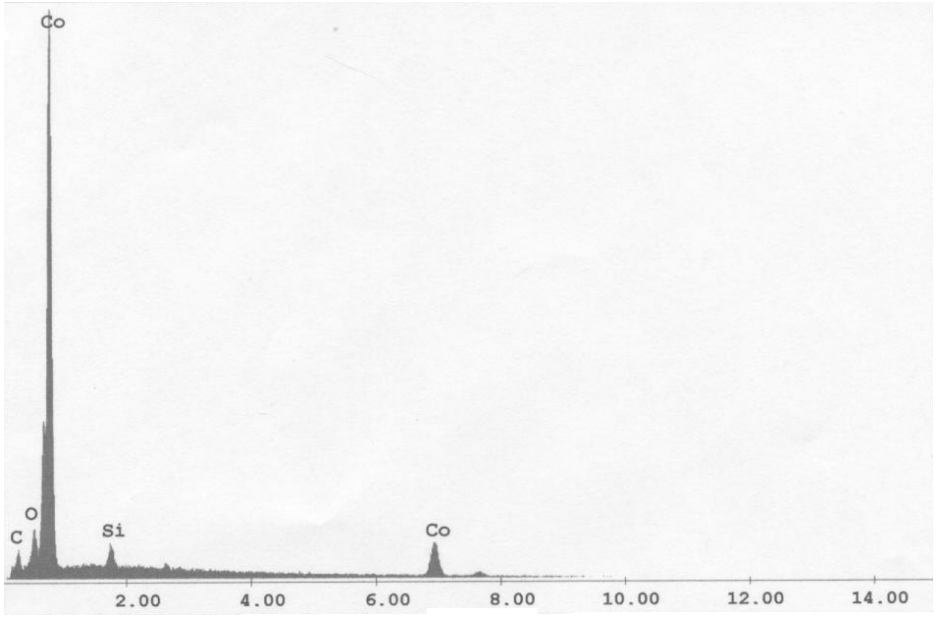

Figure **2-8**: EDAX spectra of Co-PPX 60 min cobalt bath time sample.

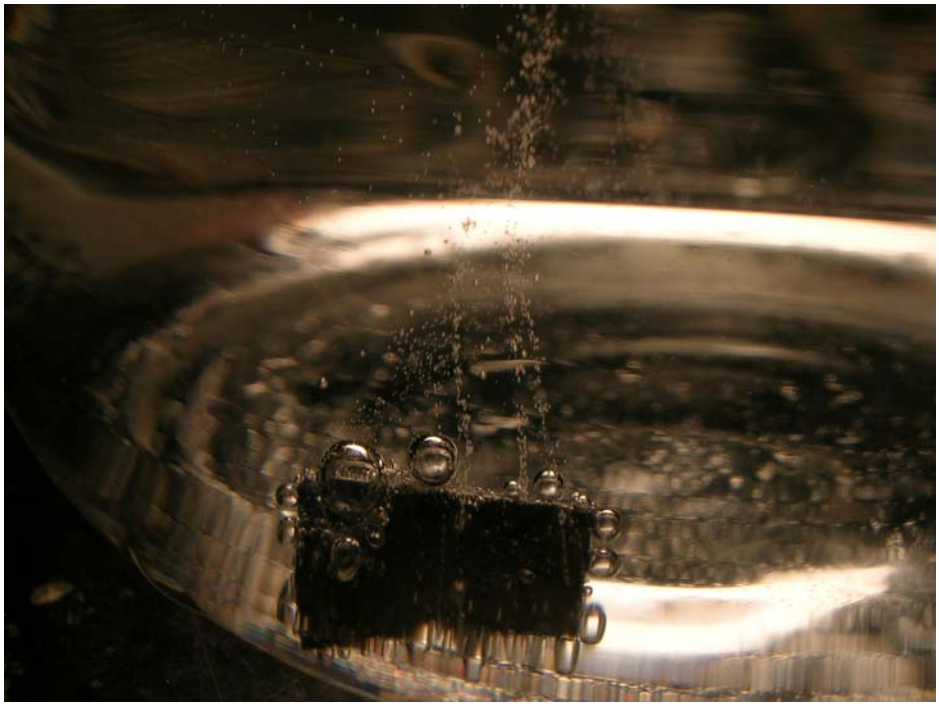

Figure **2-9**: Hydrogen generation by the nano structured Co catalyst (1% NaOH, 2.5% $NaBH_4$, 20°C)

When the catalysts are in contact with the alkaline stabilized $NaBH_4$ solutions, the hydrogen gas evolves by hydrolysis reaction. There are preferential sites on the catalyst surface for the gas to evolve. At some sites the hydrogen evolutions are active, releasing small size bubbles as shown in Figure 2-9. At other sites the catalytic reactions are not active resulting in a growth of bubbles which are adhered on the surface of the catalyst. It is thought that the differences in nano-size morphology of the catalyst layer, which are shown in Figure 2-7 (a) and (b) result in the preferential site for hydrogen generation. Also, the bubbles which are formed on the surface of catalysts are hindering the access of electrolytes ultimately reducing the hydrogen generation rate. It is also possible that the bubbles may result in low precision of hydrogen measurement.

It is also important to note that oxide film formation on the surface of cobalt catalyst in an alkaline solution is a factor that affects the hydrogen release rate. The color of Co-PPX film turned yellowish brown after the experiment. This may be due to the formation of an oxide layer in the solutions. In high alkaline solutions, the cobalt hydroxide ($Co(OH)_2$) forms on the cobalt surface. The color of $Co(OH)_2$ is known as brown, which is similar to the observation mentioned above. The discussion about new film formation on the surface of Co-PPX films and its catalytic activity of hydrogen generation will be covered in Chapter Three.

Figure **2-10** shows the hydrogen release rate of a stabilized alkaline solution of $NaBH_4$ from the cobalt surface under different conditions. Figure 2-10 (a) shows an asymptotically increasing trend with respect to the amount of cobalt. Three films were tested for each bath time, and error bars show the standard deviation of hydrogen release rate between samples. Initially, the cobalt deposited on the nanostructured PPX-Cl films

was insufficient to show any catalytic activity. However, as the cobalt deposition proceeded, the roughness of the surface increased and so did the hydrogen release rate.

A 240 minute bath time cobalt PPX catalysts showed the highest hydrogen generation rates. Figures 2-10 (b) shows the dependence of the hydrogen release rate for $NaBH_4$ concentration. The hydrogen release rate may not be dependent on the concentration of $NaBH_4$. Figure 2-10 (c) shows the hydrogen release rate dependence on the pH. The maximum rate of hydrogen release is obtained at 2.5% of $NaBH_4$ concentration and at pH 11.5. There were huge deviations in catalytic activities of 60, 120 and 240 minute samples. Among the 60min samples, some of them achieved a hydrogen generation rate of 0.395 ml/(min*cm^2), which is the highest result among the samples. This may be due to the catalytic reaction of Pd, which is used in the metallization process, possibly exposed to the solutions by delamination or cracking of the cobalt catalyst layer in the $NaBH_4$ solutions. Although Pd was not detected in the EDAX data before the hydrogen generation experiment, it is possible that cracks are formed on the cobalt layer in the alkaline stabilized $NaBH_4$ solutions. Pd itself is not good catalyst for $NaBH_4$ hydrolysis [23], however, Pd–Co may be effective in producing hydrogen with $NaBH_4$ solutions. Pd-Co catalysts are being investigated for oxygen reduction reaction [24]. Two other possible reasons for the large discrepancy could be the uneven polymerization of PPX-Cl film or metallization of cobalt. If a very conformal polymerization could be achieved, reproducible results of high hydrogen generation rates could be obtained.

The reusability of the cobalt catalyst deposited on the PPX films was tested under identical experimental conditions (2.5% $NaBH_4$ and 1% NaOH at room temperature and

pressure). The cobalt film was washed with water and dried with N_2 after each hour cycle. The hydrogen release rate for a 240 minute sample showed 8% variation in the catalytic activity during four cycles.

The hydrogen generation rates are presented in area units in this work. In most of the literatures the rates are in mass units – ml/(min*$g_{catalyst}$). In order to compare the catalyst performance of Co PPX-Cl catalyst with other catalyst developed previously, the unit conversion in mass unit is essential. However, the calculation of the Co catalyst on the PPC-Cl films is not easy because of residual water in polymer films. Also, in the absence of a standardized method of catalyst mass calculation, a comparison of hydrogen generation rate of catalysts may not be accurate.

The mass of cobalt deposited on PPX-Cl substrate was calculated by the following method. Performing a theoretical calculation of the rate in ml/(min*$g_{catalyst}$), considering the thickness of the cobalt film of 50 nm [18] and a density of cobalt (8.9 g/cm3) gives a value of approximately 10,100 ml/(min·$g_{catalyst}$). The value is the highest hydrogen generation rate of a 60 minute cobalt deposition time sample. The weight of cobalt films was measured and hydrogen generation rates in mass units (ml/(min*$g_{catalyst}$) were obtained. The hydrogen release rate varied between 2000 and 4250 ml/(g.min).

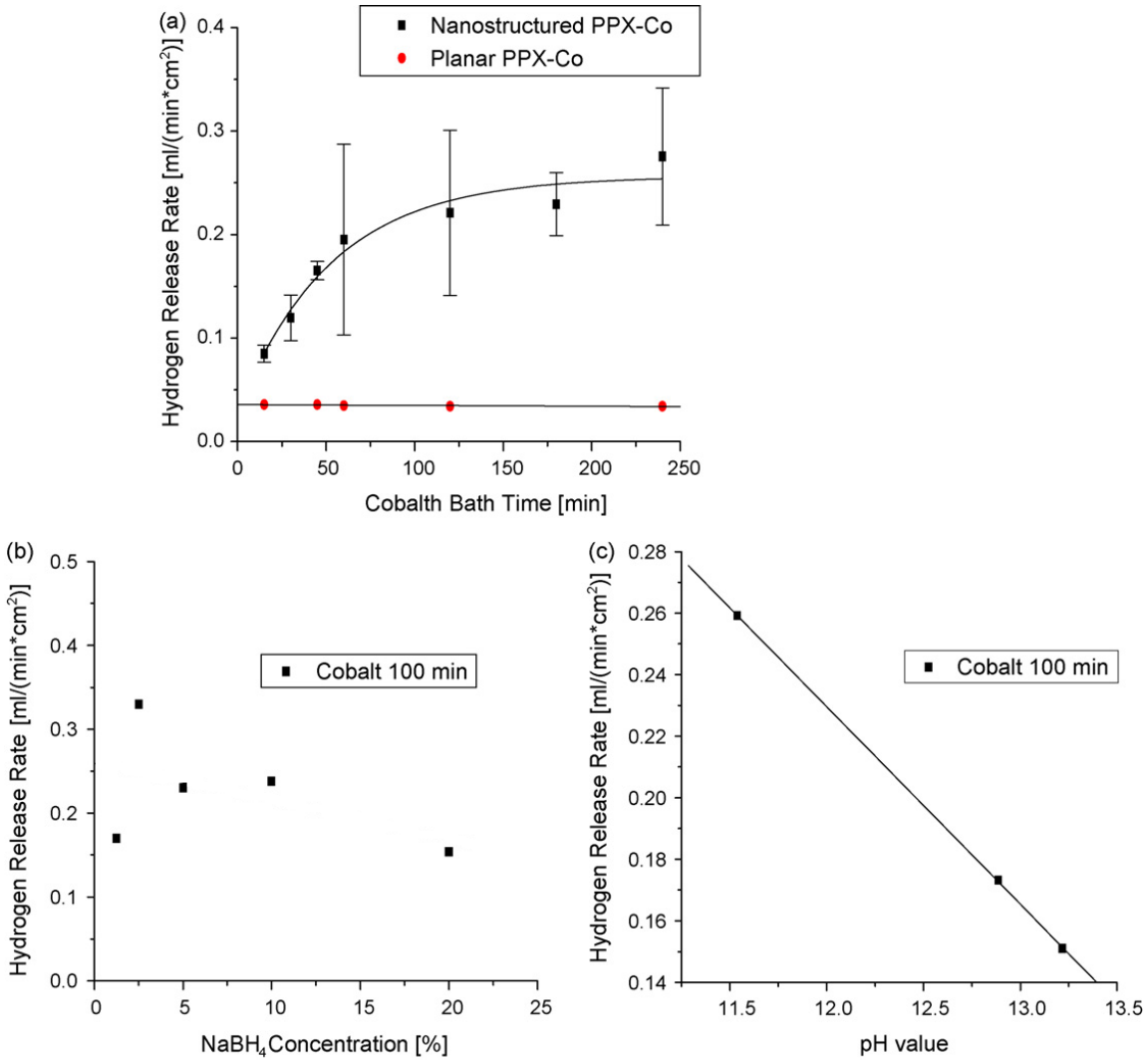

Figure **2-10**: (a) The hydrogen release rate (ml/(min*cm^2)) from the nanoporous and planar cobalt surface measured in 2.5% NaBH4 and 1% NaOH at 25 ˚C. (b) Hydrogen release rate dependence on NaBH4 concentration measured for a 100-min bath time sample at a pH of 11.5 and at 25 ˚C. (c) Hydrogen release rate dependence on pH measured for a 100-min bath time sample with 2.5% NaBH4 concentration at 25 ˚C [22].

It should be noted that the hydrogen release rate measured by volume is significantly higher compared to that of a metallic cobalt catalyst (i.e., 32 ml/(min*$g_{catalyst}$) published in the literature [22]). Some of the prominent hydrogen generation rate data published in literatures is presented in Table **2-1**. Other metal-based catalysts, such as platinum and ruthenium, show higher release-rates than the results (Table **2-1**). The facile preparation technique, with comparable release rate results, shows great promise for future development in this area.

Table **2-1**: Hydrogen generation rate of catalysts from alkaline stabilized $NaBH_4$ solutions in various conditions [22].

Catalyst	$NaBH_4$ concentration (wt. %)	NaOH concentration (wt. %)	Hydrogen release rate (ml/(min·$g_{catalyst}$))	Temperature (°C)	Reference
A-26 (Ru based)	20	10	4032	25	[25]
IRA-400 (Ru based)	12.5	1	~9600	25	[13]
Pt/C	10	5	23,090	N/A	[26]
CoB	2	5	~3500	15	[27]
Pt-LiCoO2	5	5	~24000	25	[28]
CoB	25	3	~7500	25	[29]
Co/PPX-Cl	2.5	1	4250	20	This work

2.4 Conclusions

The cobalt deposited nanostructured PPX films exhibited excellent catalytic activities over the planar PPX films. The hydrogen generation rate increased as a function

of deposition time of PPX film in cobalt bath. The hydrogen generation rates follow logarithmic trends; therefore, a 240-minute bath time cobalt PPX catalysts showed the highest hydrogen generation rates. In contrast to the nanostructured PPX films, the planar PPX films exhibited poor rates of hydrogen generation. The influence of cobalt bath deposition time of Co planar film was not observed as expected. The hydrogen generation rates of Co-planar PPX films were almost constant regardless of various cobalt bath deposition times. The variations in hydrogen generation rates were observed. To identify the reasons for variations in results, more research needs to be conducted in the future. Some recommended works for resolving this problem are suggested in Chapter Five.

Chapter 3

STUDY OF COBALT AS INEXPENSIVE AND EFFECTIVE CATALYST FOR THE PRODUCTION OF HYDROGEN IN ALKALINE STABILIZED SODIUM BOROHYDRIDE SOLUTIONS

3.1 Introduction

As discussed in Chapter Two, the color of the cobalt PPX catalyst immersed in an alkaline solution containing NaBH4 changed color, immediately after the sample hydrogen generation occurred. It changed from its original silver color to a dark brown color.

The thermodynamic stability information of cobalt in aqueous systems can be obtained from Pourbaix diagram, which is also known as E-pH diagram. The Pourbaix diagram of cobalt – water system is shown in Figure **3-1**.

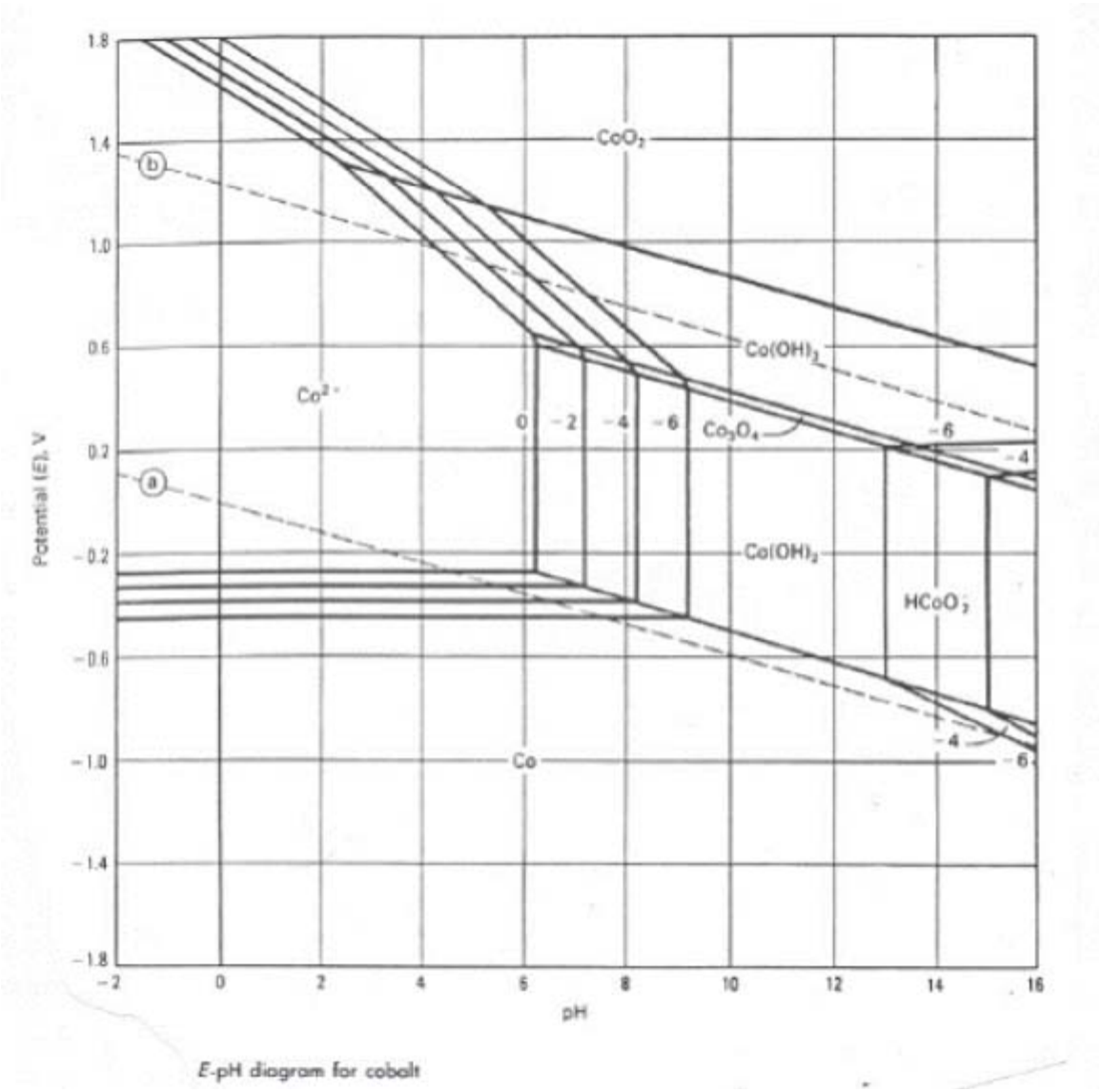

Figure **3-1**: Pourbaix diagram of cobalt in water at 25°C [30].

The literature established that the change on color of the cobalt PPX sample after the immersion in the solution (0.677 M of NaBH4 and 0.241 M of NaOH) might be due to the formation of an oxide layer. It is reported [31] that the brown color is due to β-$Co(OH)_2$ as the CoOOH forms. The oxidation of cobalt depends on the pH of the aqueous

solutions [32]. According to the study by Badawy et al, the formation of the cobalt oxide film in basic solutions can be explained by the following reactions:

$$[CoOH]^{+} + OH^{-} \rightarrow Co(OH)_2 \quad (\mathbf{3\text{-}1})$$

$$Co(OH)_2 + OH^{-} \rightarrow CoOOH + H_2O + 2e^{-} \quad (\mathbf{3\text{-}2})$$

$$3CoO + 2OH^{-} \rightarrow Co_3O_4 + H_2O + 2e^{-} \quad (\mathbf{3\text{-}3})$$

It is reported that the α-$Co(OH)_2$ (blue color) is formed by covalently bonded tetrahedral coordinated Co^{2+} ions in the intermediate layers of the oxide. The red color of β-$Co(OH)_2$ is a consequence of Co^{2+} ions in octahedral coordination. If Co (II) salts are in excess during deposition, the resulting α-$Co(OH)_2$ may appear green instead of blue (not observed in these experiments). Partial oxidation can influence the color of α-$Co(OH)_2$ towards green, while partially oxidized samples of β-$Co(OH)_2$ appears in brown tones [31]. When the pH is in the range of $9 < pH < 14$, the color of the β-$Co(OH)_2$ turns brown with the formation $Co(OH)_3$. The β-$Co(OH)_2$ changes color from light pink to dark brown as the CoOOH forms.

Experiments on cobalt in potassium hydroxide solutions alone conducted by Ismail et al. [33] revealed the structure of oxide film by x-ray photoelectron spectroscopy (XPS). They concluded that the cobalt oxide film is composed of two layers: inner layer of α-$Co(OH)_2$ and CoO, outer layer of CoOOH.

(a) (b)

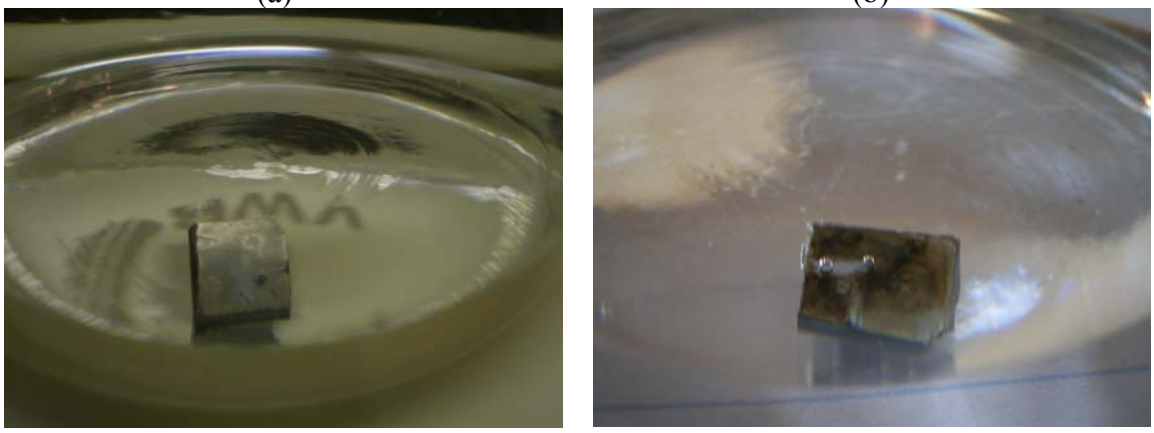

Figure **3-2**: Cobalt PPX film in deaerated alkaline solutions (pH = 12.885, T = 20°C). The color change of cobalt PPX-Cl film indicates the formation of oxide films on the surface of catalyst. (a) : initial state and (b) : 93 hours later.

The oxide films, CoOOH or a mixture of β-$Co(OH)_2$, CoOOH and Co_3O_4, may affect the properties of the catalyst resulting in a decrease of the catalytic activities. It is also possible that in naturally aerated (i.e. O_2 is dissolved in the electrolyte) or deaerated solutions the decrease in the catalytic activity due to oxidation can be avoided by adding organic inhibitors that protects the catalyst.

In a strong alkaline deaerated environment (pH>13), cobalt hydroxide in a 0.261M NaOH and 0.677M NaBH4 electrolyte will not react to grow a film (see Figure 3-1 area between 12.5< pH< 13.5 and equilibrium potential between the dotted line (a) and line at -1.0 V_{SHE}). In naturally aerated solutions, the presence of oxygen dissolved shift the equilibrium potential of the cobalt dissolution reaction some place between the dotted line (b) and -1.0 V_{SHE} where at approximately pH 13 there are many oxide films that can co-exist ($Co(OH)_3$, CO_3O_4, $CO(OH)_2$) and Co could dissolve as $HCoO2^-$ depending on the exact value of the equilibrium potential. It is thought that in the morphology of a nanostructured substrate, where the spikes and valleys are composed of

changes the local potential of cobalt to a positive direction - probably in the range of -0.5 to -0.25 V_{SHE} - forms the $Co(OH)_2$ films on the surface of the cobalt. Therefore, the deaeration of the alkaline stabilized sodium borohydride electrolyte will drastically change the nature of the film. The passive film formation and its nature formed on the surface of the cobalt catalyst - in an alkaline solution - will affect the color changes of the catalyst surface and the hydrogen generation rates.

Accordingly, from the literature and the experimental observation, I postulated that a double layer is formed on the cobalt surface catalyst. The layer close to the metal surface is believed to be a compact thin film and a second re-precipitated layer is believed to form on top of the compact thin film. I explored this hypothesis by suppressing the re-precipitated film through the use of ethylenediaminetetra acid (EDTA).

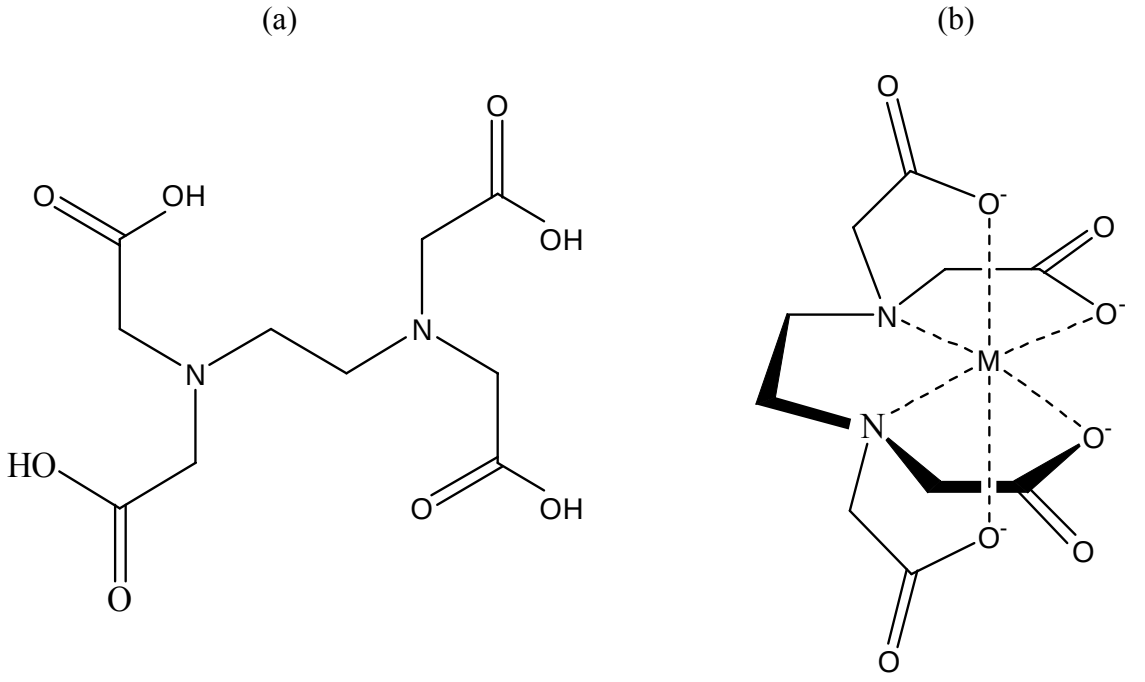

Figure **3-3**: Structure of EDTA (a) and Metal-EDTA chelate (b).

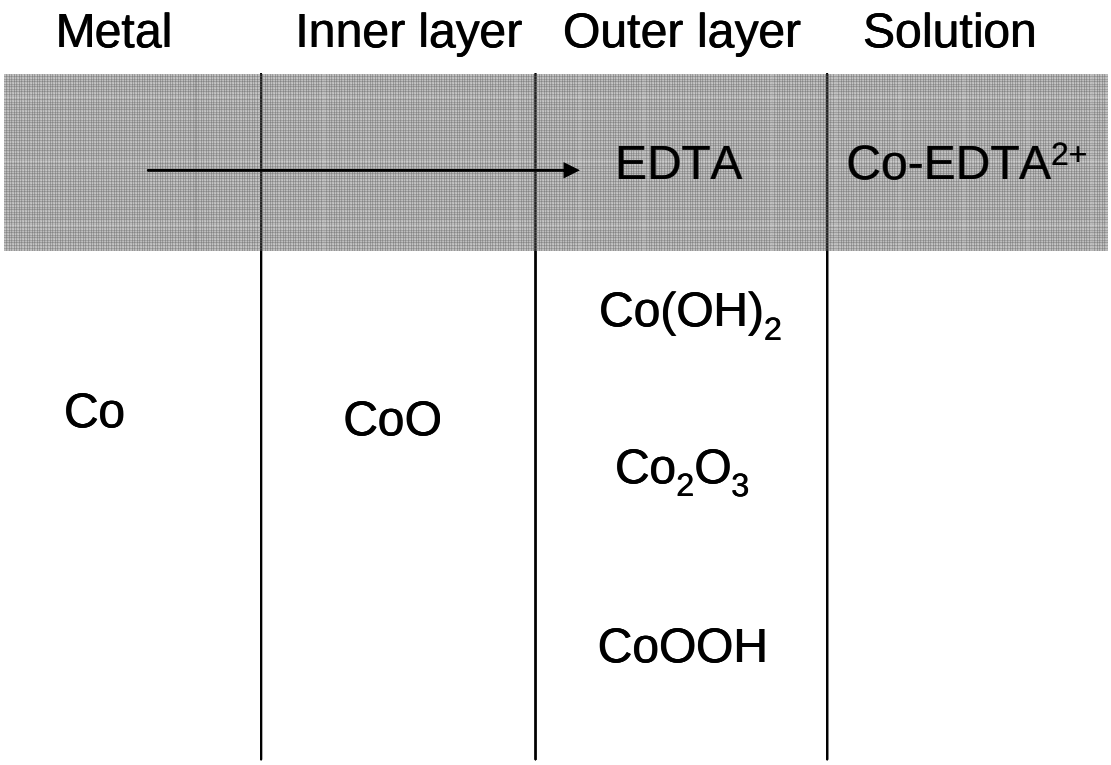

Figure **3-4**: Proposed schematic of passive films on cobalt in alkaline solutions. It is assumed that Co-EDTA chelate prevent the formation of outer oxide layer in the presence of EDTA. The formation of CoOOH, Co_3O_4 may depend on the potential of sample.

3.2 Experimental Procedure

3.2.1 Corrosion Potential

A three-electrode electrochemical cell was used to measure open circuit potentials as shown in Figure **3-5**. The working electrode used was a cobalt rode (99.95%, Alfa Aesar) placed inside epoxy resin (Metlab Corp.). The working electrode was mechanically polished, washed thoroughly with DI water. Graphite was used as a counter electrode and saturated calomel electrode (SCE) placed in a luggin pillar filled with

electrolyte was used as a reference electrode. Then, 2.5 % $NaBH_4$ (0.677 M) solutions stabilized by 1 % NaOH (0.261 M) were used as electrolytes. The solutions were deaerated for 30 minutes with nitrogen gas (ultra high purity) before the open circuit potential (OCP) measurements. The OCP of cobalt in the electrolyte was measured, versus the calomel electrode reference, for approximately an hour. The OCP of cobalt electrode in 0.261 M NaOH solutions were also measured versus the same reference electrode.

3.2.2 EDAT Effect

Cobalt powder (Alfa aesar, 99.8%) with a diameter of 1.6 μm was used as a catalyst for the hydrolysis of alkaline stabilized sodium borohydride solutions. ACS grade chemicals of sodium hydroxide (EMD, 97%, ACS grade) and sodium borohydride (Alfa aesar, 97%) were used. To investigate the effect of EDTA, 125 ml of 1 wt.% NaOH, 2.5 wt.% $NaBH_4$ solutions with and without EDTA were prepared. For the oxygen effect test, deaeration of the solutions with argon gas was carried out for 30 minutes. The catalytic activity of cobalt powder was tested by measuring the amount of hydrogen gas released. The pH and temperature of the solutions were monitored before and after each experiment and then recorded. The pH of the solutions was approximately 13, while the temperature of solutions was maintained at room temperature. The solution was contained in a 125 ml container, and the hydrogen gas generated was collected in the water column, which was immersed into a beaker. The amount of hydrogen release was recorded with respect to time. From these data, the rates of hydrogen gas generation were calculated by differentiating the volume of hydrogen gas with respect to time. The

hydrogen generation rates were measured by volume of hydrogen per grams of cobalt powder.

Figure **3-5**: Experimental setup for open circuit potential measurement.

3.3 Results

The open circuit potential (OCP) of the cobalt rod in 1% NaOH (0.227M) solutions was measured. The pH of the solutions was 13 and the OCP of cobalt was stabilized to -0.815V_{SCE} (-0.574 V_{SCE}). Moreover, the formation of oxide films on the cobalt surface was observed, as shown in Figure **3-6**. It is thought that the $Co(OH)_2$ films were formed on the cobalt surface according to the Pourbaix diagram. However, the OCP of cobalt in the solutions of 2.5 % $NaBH_4$ (0.677 M) and 1 % NaOH (0.261 M) was -1.203V_{SCE} (-0.962V_{SHE}). The high negative potential may due to the presence of $NaBH_4$, which is a reducing agent. No oxide or hydroxide film may be formed on the surface of the working electrode at pH 13 in this case. In the absence of the Pourbaix diagram of cobalt in this solution ($NaBH_4$), an exact prediction of oxide film would be impossible. Therefore, the characterization techniques would reveal the composition of films in the solutions.

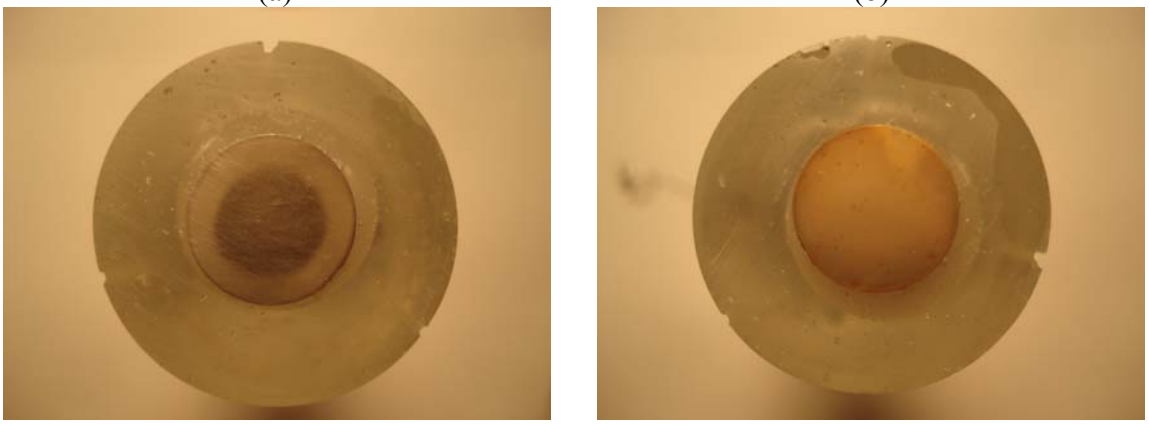

Figure **3-6**: Pictures of cobalt rod surface before (a) and after (b) 1 hour open circuit potential measurement in 0.261M NaOH solution.

The result showed that the hydrogen generation rates from the deaerated solutions were higher than the naturally aerated solutions regardless of the addition of EDTA. In the deaerated solution, the hydrogen generation rate increased about 30% when compared with naturally aerated solution. The results may imply that oxygen has an impact on the catalytic activity on hydrogen generation and this is in accordance with the hypothesis – outer oxide layer formation by oxygen in the solution prohibits the catalytic activity of cobalt.

EDTA contained solutions were less actively generated hydrogen than the solutions without EDTA regardless of naturally aerated or deaerated solutions. In deaerated solutions, adding EDTA reduced the hydrogen generation rate about 30% compared with the solution without EDTA. The case was even worse in naturally aerated solutions where the EDTA resulted in the reduction of the hydrogen generation rate by more than 50% compared with the solutions without EDTA.

The main hypothesis is that EDTA enhances the catalytic activity of cobalt by suppressing formation of a precipitate layer resulting in the enhancement of catalytic activities. However, the results showed the decrease in the hydrogen generation rate when EDTA was dissolved in the solutions. It is thought that the Cobalt – EDTA chelate may block the absorption of sodium borohydride ions on the surface of catalyst. In the absence of EDTA, diffusion of borohydride ions to the surface of cobalt might be faster than the solutions with EDTA. The serious reduction of hydrogen generation rate occurred in the presence of oxygen and EDTA in the solutions. The effect of oxygen and EDTA on the reduction seems to be combined.

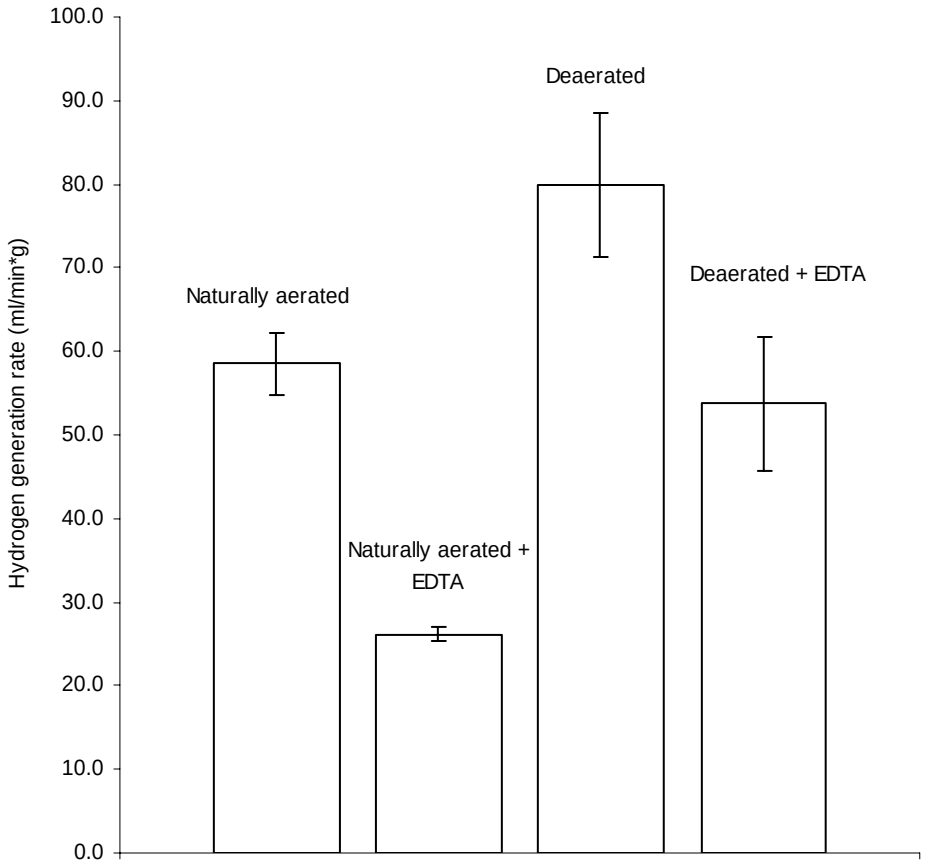

Figure **3-7**: Influence of 0.01M EDTA on hydrogen release of naturally aerated and deaerated 2.5% $NaBH_4$ solutions with 1% NaOH.

3.4 Conclusions

The effects of oxygen and EDTA were evaluated. In deaerated solutions where there is no oxygen dissolved, the rates of hydrogen generation were increased as expected. In other words, oxygen in the electrolyte decreased the catalytic activity of

cobalt in hydrogen generation. As expected, the deaeration of the alkaline stabilized sodium borohydride electrolyte changed the nature of the film. However, the exact structure of oxide film and its compositions on the surface of cobalt catalyst in both naturally aerated and deaerated solutions were not completely understood.

When EDTA was added to the electrolyte in naturally aerated solutions, the cobalt powder exhibited poor catalytic activity. EDTA did not effectively increase the hydrogen generation rates, as postulated originally. The reasons for poor catalytic activity of cobalt powder in the presence of EDTA in naturally aerated solutions were not fully understood. It is thought that Co-EDTA chelate hinders the access of $NaBH_4$ as it comes into contact with the inner cobalt passive film.

Chapter 4

STUDY OF ALUMINUM ALLOY FOR THE PRODUCTION OF HYDROGEN FROM ALKALINE STABILIZED SODIUM BOROHYDRIDE SOLUTIONS

4.1 Introduction

The activities of many metals on hydrolysis of NaBH4 are different and investigating the catalytic activity of each metal is worth doing. Thus, the purpose of this chapter is to investigate the catalytic activity of widely available metals, which is inexpensive and effective on hydrogen generation. A collection of coins was tested to screen effective catalysts for the hydrolysis of sodium borohydride by dipping them into alkaline stabilized NaBH4 solutions. Among the metal alloys, the Austrian 10 groschen (11¢ in us currency) coin showed good hydrogen generation and was therefore selected for the experiment. The composition of the coin was characterized by an energy dispersive x-ray (EDAX). The composition of this aluminum alloy is known as 98.5% aluminum and 1.5% magnesium.

Aluminum in the strong alkaline solutions reacts violently and generates hydrogen as shown in reaction 4-1. $NaAl(OH)_4$ decomposes when it is saturated and NaOH is generated by reaction 4-2 [34].

$$2Al + 6H_2O + 2NaOH \rightarrow 2NaAl(OH)_4 + 3H_2 \qquad (\mathbf{4\text{-}1})$$

$$NaAl(OH)_4 \rightarrow NaOH + Al(OH)_3 \qquad (\mathbf{4\text{-}2})$$

Studies on hydrogen generation by the reaction of aluminum in alkaline solutions have been investigated. A study of the use of aluminum and its alloy in hydrogen generation with the combination of hydrolysis of $NaBH_4$ has been investigated [35]. The investigation revealed that the use of sodium borohydride with alkaline solutions has a synergetic effect on hydrogen generation, due to the increased corrosion rate of aluminum by hydrolysis of sodium borohydride. However, it should be noted that the hydrogen generation rate of aluminum in a saturated $Ca(OH)_2$ solution was higher than that of aluminum in the $NaBH_4$ added $Ca(OH)_2$ solutions. Cathodic evolution of hydrogen was studied by Macdonald et al [36]. Aluminum and its alloys were investigated as anodes in aluminum-air batteries. The goals of their work were to understand the electrochemical behavior of aluminum alloys in high alkaline solutions (4M KOH) and establish information about parameters for hydrogen evolution.

The hydrogen generation of the aluminum alloy was evaluated. The effects of EDTA chelating and the oxygen effect dissolved in the solution were investigated. As the E-pH diagram was used to explain the state of cobalt in an aqueous system, it is useful to investigate the behavior of aluminum in the system. The Pourbaix diagram of pure aluminum is shown in Figure 4-1. Although the diagram is for pure aluminum, it is used as a tool for the interpretation of the aluminum magnesium alloy, with the understanding that the alloy's main component is aluminum (98.5%).

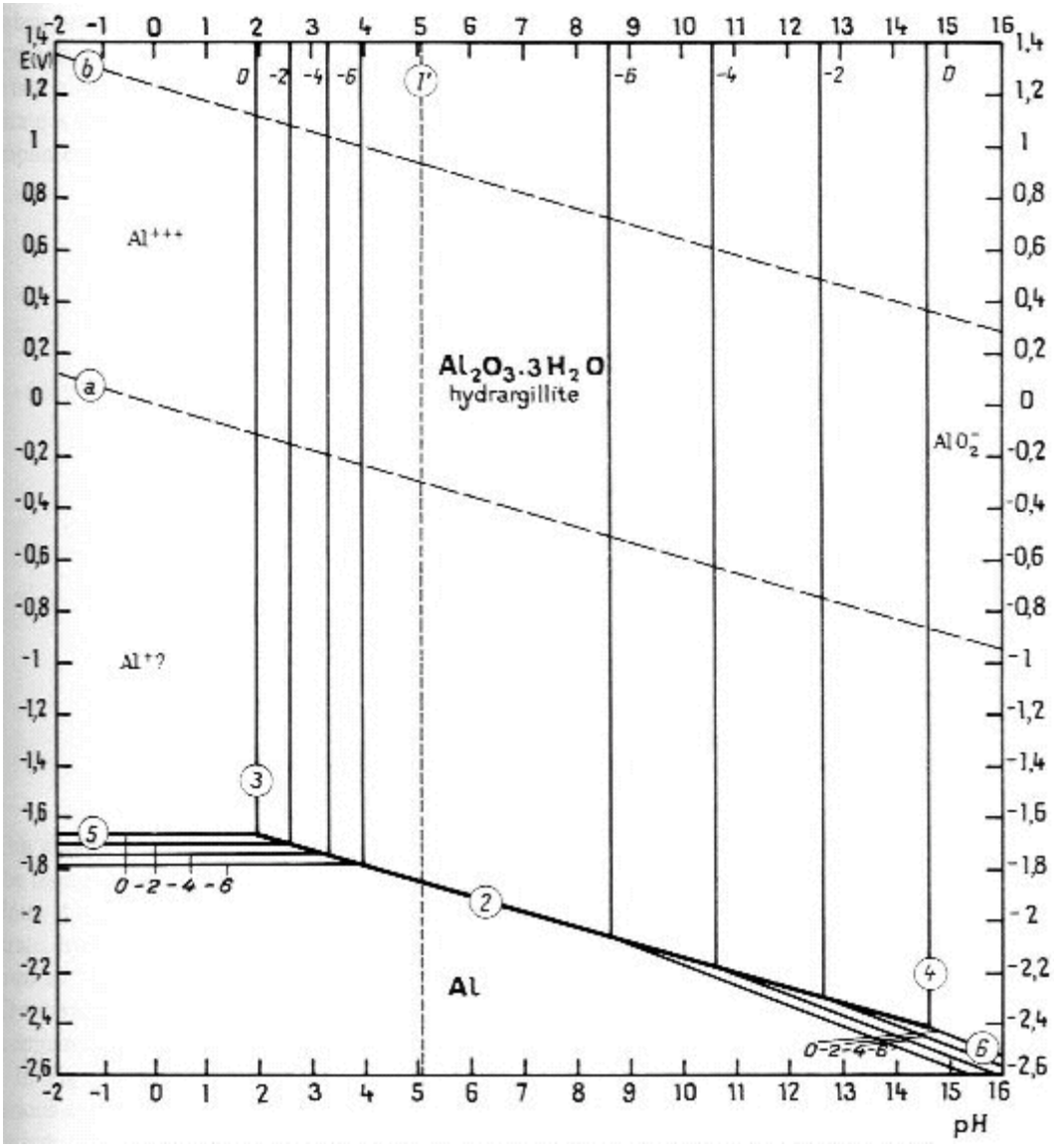

Figure **4-1**: Pourbaix diagram of aluminum-water system at 25°C [30].

4.2 Experimental

4.2.1 Characterization of aluminum alloy

All chemicals used are reagent grade. Aluminum alloy was chosen for the experiment because of its availability and catalytic activity for hydrolysis of $NaBH_4$. The composition of the alloy is known as 98.5% aluminum and 1.5% magnesium. The diameter of the alloy is 20mm and the area of the alloy is 3.14 cm^2. The alloy's composition was characterized by energy dispersive x-ray (EDAX) on Philips XL-30 scanning electron microscope (SEM) at an ambient temperature.

4.2.2 Corrosion Potential

The set up for the corrosion potential measurement of the sample was essentially the same as in the Chapter Three. A three-electrode electrochemical cell was used to measure open circuit potential as shown in Figure **3-5**. The working electrode used was the aluminum alloy (98.5% Al, 1.5% Mg) placed inside epoxy resin (Metlab Corp.). The working electrode was mechanically polished, washed thoroughly with DI water. Graphite was used as a counter electrode and a saturated calomel electrode (SCE) placed in a luggin pillar filled with electrolyte used as a reference electrode. 2.5 % $NaBH_4$ (0.677 M) solutions stabilized by 1 % NaOH (0.261 M) were used as electrolytes. The open circuit potential (OCP) of cobalt in the electrolyte was measured versus calomel electrode reference for approximately one hour. The OCP of cobalt electrode in 0.261 M NaOH solutions was also measured versus the same reference electrode. The measured potential for a 0.261M NaOH and 0.677M NaBH4 electrolyte was stabilized at approximatly -

0.775 V_{SCE} (-0.574 V_{SHE}) at pH 13. In a 0.261M NaOH electrolyte the OCP was stabilized at approximately -0.95 V $_{SCE}$ (-0.709 V_{SHE}). Supposedly, the aluminum dissolves into the electrolyte as Al_2O in both cases. And due to the dissolution of aluminum in the electrolyte the surface of the aluminum alloy will be bare aluminum.

4.2.3 Effect of NaOH concentration and EDTA

The sample was placed in epoxy resin for easy sample preparation for the experiment. Figure 4-2 shows the schematic of the sample. Mechanical polishing of the sample was carried out before the hydrogen generation measurement to remove undesirable layers formed on the surface of the alloy. The sample was prepared by polishing the surface with medium roughness with 600 grid grind paper and cloth rubbing with1μm alumina power solution (Metlab Corp.). The alloy was then washed with deionized water and dried with nitrogen gas.

The solutions with the different concentration of NaOH (1, 5, 10 and 15 wt.%) were prepared to investigate the effect of NaOH concentration. The concentration of the $NaBH_4$ was 2.5wt.% for all the experiments. To investigate the effect of the oxygen dissolved in the solution both naturally aerated and deaerated solutions were prepared. Aqueous solutions of 2.5 % $NaBH_4$ (0.677 M) and 1 % NaOH (0.261 M) were used to investigate the effect of EDTA and oxygen. The pH and temperature of the solutions were monitored before and after each experiment and then recorded. The pH of the solutions used were approximately 13, while the temperature of solutions was maintained at 19 ~23 ºC. The solution was contained in the 125 ml container, and the hydrogen gas generated was collected in the water column, which was immersed into a beaker. The

amount of hydrogen release was recorded with respect to time. From these data, the release rate was obtained by differentiating the hydrogen release volume with respect to time. The hydrogen release rate was measured by volumes of hydrogen gas per unit area of aluminum alloy.

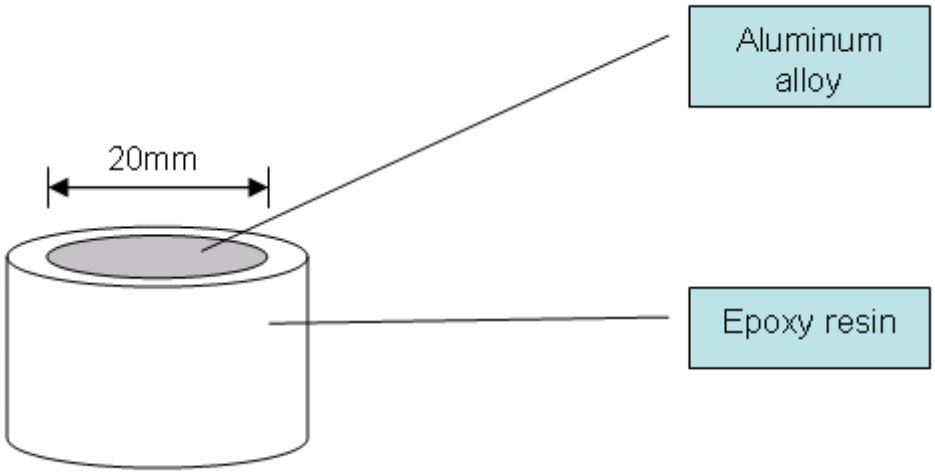

Figure **4-2**: Aluminum alloy examined as a catalyst for hydrolysis of sodium borohydride. The sample was hold in epoxy resin for sample preparation.

4.3 Results

The composition of the aluminum alloy was analyzed by EDAX and the result is showed in Figure 4-3 and Table **4-1**.This result is consistent with the known composition, which is 98.5 % aluminum and 1.5% Mg, when the oxide is considered from the result.

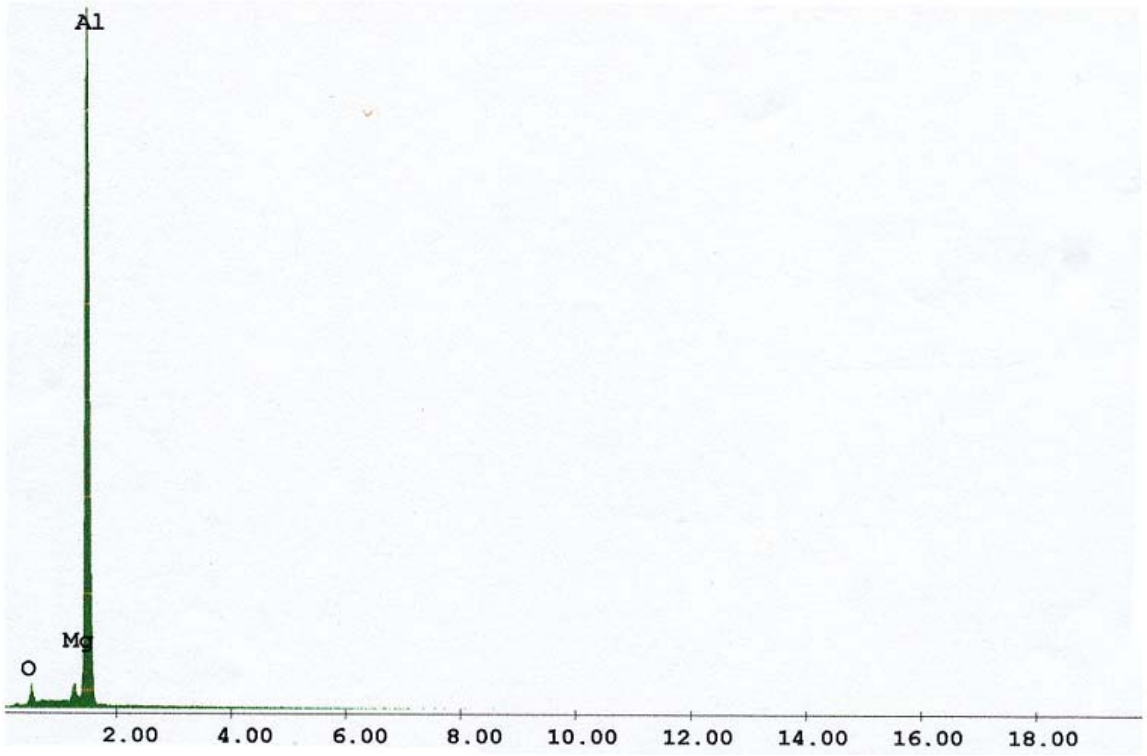

Figure **4-3**: Energy dispersive x-ray result showing composition of aluminum alloy

Table **4-1**: EDAX ZAF quantification (standardless) of Al alloy.

Element	Wt %	At %	K-Ratio
O K	3.26	5.38	0.0178
MgK	1.44	1.56	0.0149
AlK	95.30	93.07	0.9357
Total	100.00	100.00	

Element	Net Inte.	Bkgd Inte.	Inte. Error	P/B
O K	12.74	2.19	3.12	5.81
MgK	10.47	11.96	5.39	0.88
AlK	605.17	9.26	0.40	65.32

In the hydrogen generation by aluminum, the role of aluminum is different from the hydrogen generation when using cobalt. Cobalt is a catalyst that is not involved in the production of hydrogen. On the contrary, aluminum dissolves in high alkaline solutions and reacts with water and sodium hydride. Figure **4-4** shows the hydrogen generation (ml/cm^2) from aluminum in alkaline stabilized sodium borohydride solutions as functions of time and NaOH concentration. Figure **4-5** indicates hydrogen generation rates ($ml/min \cdot cm^2$) from the data given in figure 4-4. The hydrogen generation rate was highest at the NaOH concentration of 10 wt. % while a 15wt.% NaOH solution showed a lower hydrogen generation rate than 10wt.% solutions. The increase of NaOH concentration in the solution increases the available NaOH ions for the hydrogen generation reaction. The decrease in hydrogen generation rate of 15% NaOH solution might be due to the high viscosity of solutions resulting in a decrease of ions diffusion in the solutions. In the evaluation of the oxygen effect on the hydrogen generation, the differences between naturally aerated and N_2 gas deaerated solutions in hydrogen generation rates were not noticeable. This result means that oxygen dissolved in the solutions is not a rate determining factor on hydrogen generation of the aluminum alloy. This might be due to the continuous dissolution of the aluminum alloy and the fact that the oxide film had no chance to form on the surface of the alloy.

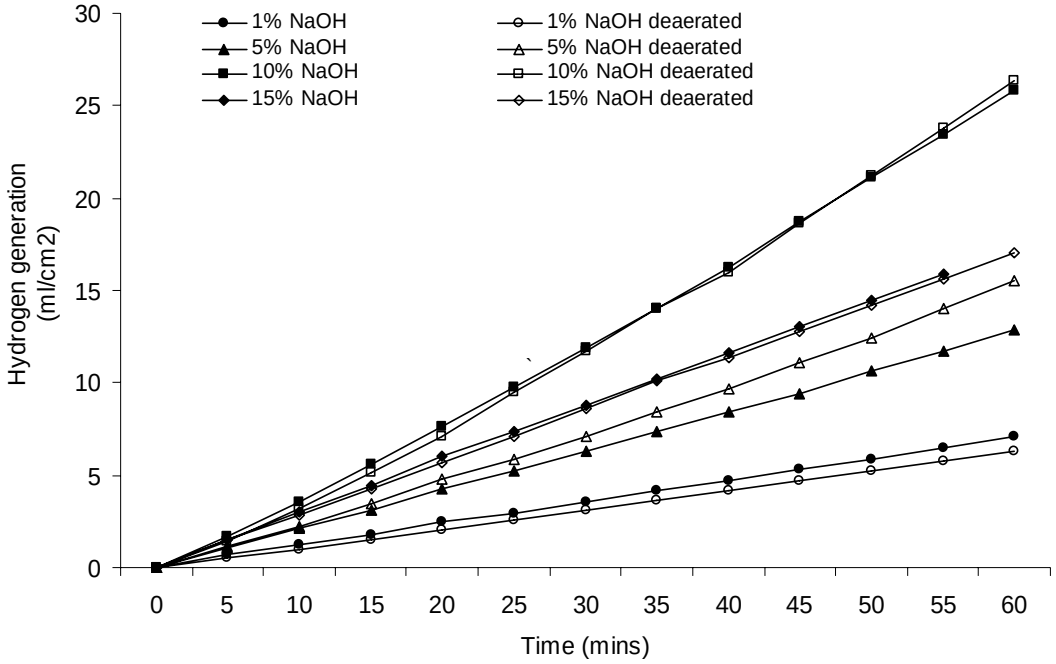

Figure **4-4**: The effects of NaOH concentration and deaeration on hydrogen generation of Al alloy. 1, 5, 10, 15 % NaOH, 2.5% $NaBH_4$ solutions with naturally aerated and deaerated (N_2) solutions were used at 19~23°C.

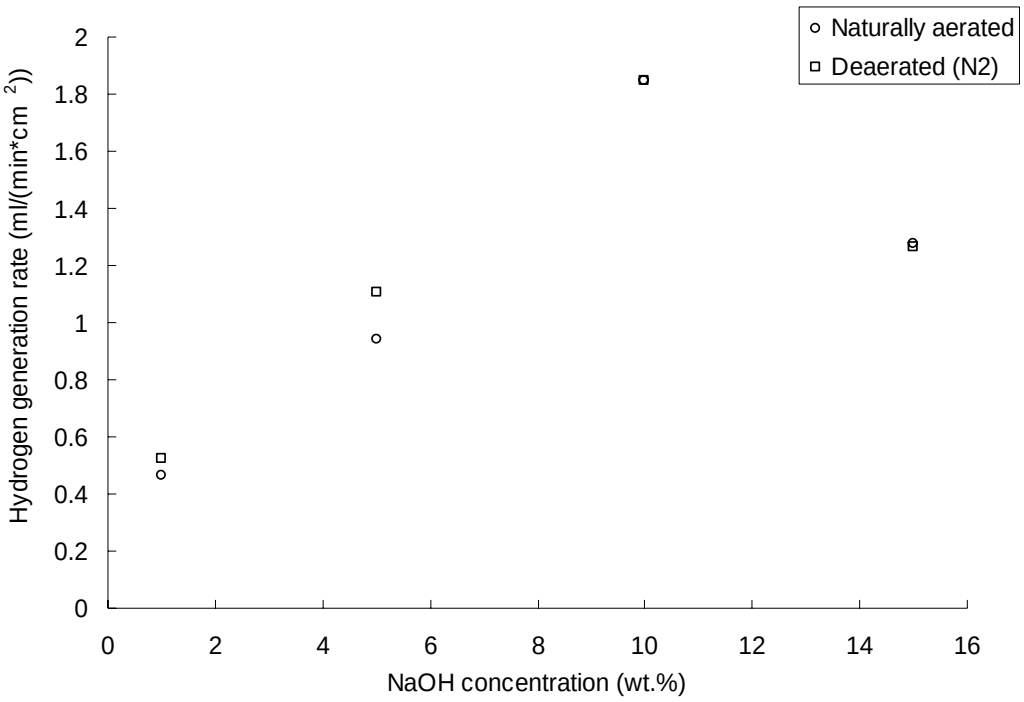

Figure **4-5**: The effects of NaOH concentration (1, 5, 10 and 15 wt.%) and deaeration of solutions at 19~23°C. Each solutions contains 2.5 wt% $NaBH_4$.

The result showed that the hydrogen generation rates in naturally aerated solutions are almost the same as deaerated solutions shown in Figure **4-6**. The higher hydrogen generation rate was achieved in both naturally aerated and deaerated solutions with EDTA. Supposedly, EDTA dissolved in the solutions increased dissolution rate of aluminum, which resulted in the higher hydrogen generation rate. The increase of hydrogen generation rate was also observed with EDTA dissolved and deaerated solutions.

However, the hydrogen generation rates of both deaerated solutions with and without EDTA were somewhat lower than that of naturally aerated solutions. The small difference in the hydrogen generation rate between naturally aerated and deaerated

solutions could be interpreted as a factor that oxygen did not affect the rate of hydrogen generation. It is consistent with the result of the NaOH concentration effect test shown in Figures 4-4 and 4-5.

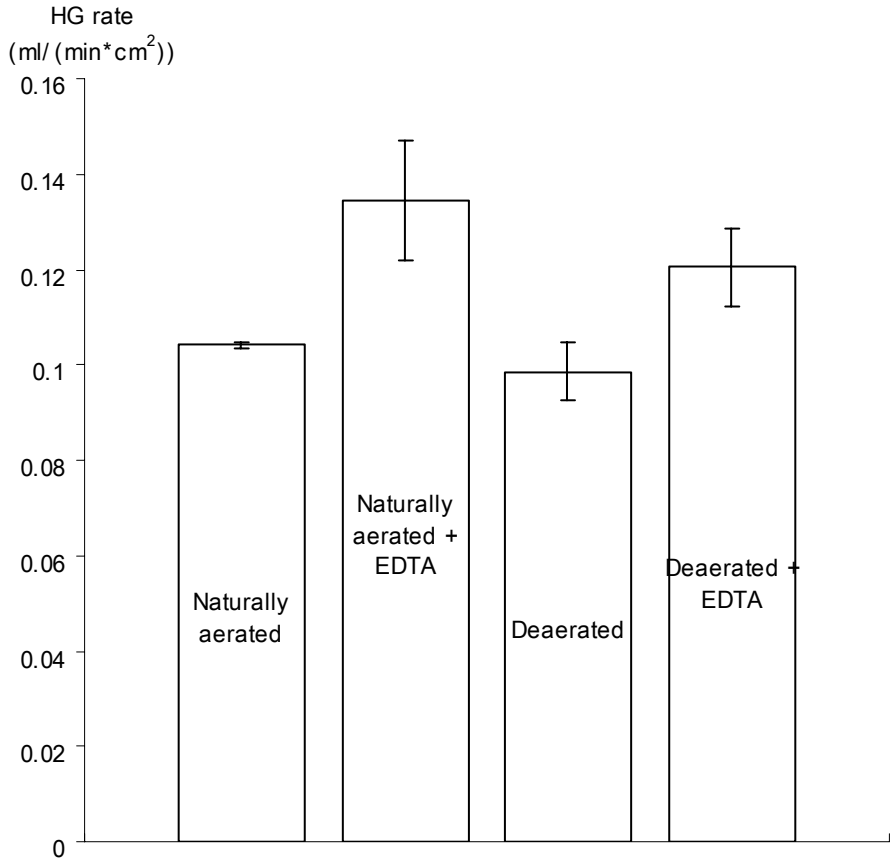

Figure **4-6**: Hydrogen generation rate of Al alloy sample in 0.261M NaOH, 0.677 M $NaBH_4$ solutions at 20°C.

Hydrogen generation from NaOH without sodium borohydride was tested to examine the hydrogen generation through the reaction of aluminum and sodium hydroxide alone. By comparing the results in Figures 4-6 and 4-7, the conclusion is that most of the hydrogen in 0.261M NaOH and 0.677M $NaBH_4$ solutions comes from the

reaction of aluminum and sodium hydroxide. And also, the hydrogen generation rate was lower than the NaBH4 dissolved solutions. Therefore, it can be concluded that the hydrogen can be generated from two reactions - hydrolysis of $NaBH_4$ and reaction of Al and NaOH. The result is in well accordance with the work in the literature [35] insisting that the hydrolysis of $NaBH_4$ increases the hydrogen generation rate by increasing corrosion of aluminum in alkaline solutions.

The formation of films on the aluminum alloy surface was observed. Figures **4-8** show the pictures of the sample before and after the experiment. The change in the sample after the experiment was observed. It is predicted that there might be a residue of $Al(OH)_3$ on the alloy surface and/or formation of film composed of sodium and borate due to the presence of $NaBH_4$ in the solutions. The color of film formed on the sample surface was brown and the film was not homogeneously formed. However, the composition of film and its effect on the hydrogen generation rates should be investigated in the future.

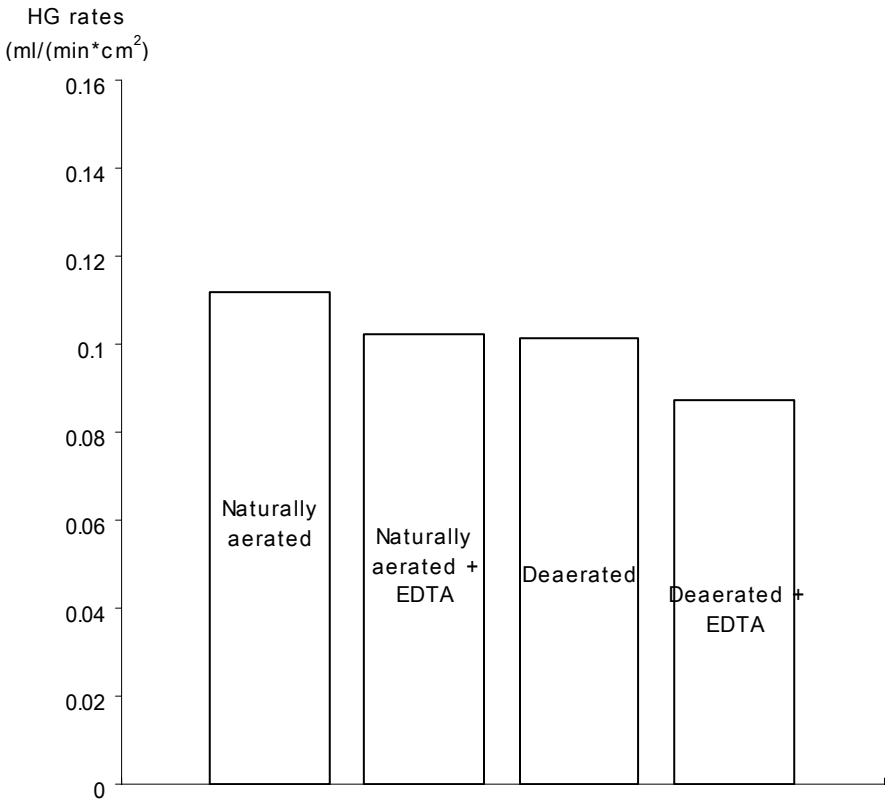

Figure **4-7**: Hydrogen generation from aluminum in 0.26M NaOH solutions at 20°C.

(a) (b)

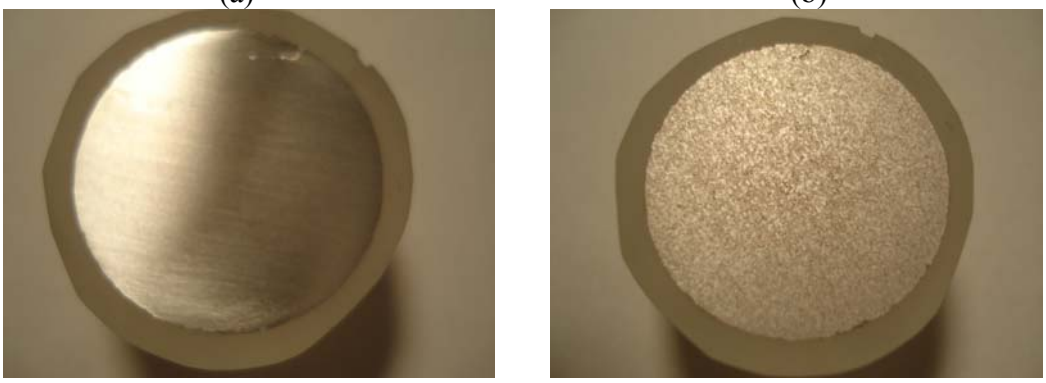

Figure **4-8**: Aluminum alloy catalyst before (a) and after (b) one hour hydrogen generation experiment in alkaline (pH=13) stabilized 2.5% $NaBH_4$ solution. (T = 20°C)

4.4 Conclusions

The aluminum alloy as a source of hydrogen and its catalytic activity for hydrolysis of sodium borohydride has been studied. Through the dissolution of aluminum in the alkaline solutions, hydrogen gas was generated by the reaction of aluminum with sodium hydroxide. The NaOH concentration effect was studied and it is concluded that the optimized concentration of 10% NaOH produced maximum hydrogen gas in the range of 1 ~ 15 wt. % NaOH concentration. It is thought that the high concentration of NaOH increased the reaction rate of hydrogen generation.

The effect of EDTA on hydrogen generation was also studied. The addition of EDTA increased the hydrogen generation rate of aluminum alloy in 1 wt. % (0.261M) NaOH, 2.5% (0.677M) $NaBH_4$ solutions with and without deaeration. The results showed that the EDTA increased the rate of hydrogen generation about 30% regardless of deaeration. It is thought that the dissolution of Al by EDTA increases the concentration of Al in the solution resulting in the increase of hydrogen generation.

The hydrogen generation reaction of Al alloy with 1 wt. % (0.261M) NaOH solutions was investigated for the comparison of the hydrogen generation rate with the solutions of 1 wt. % (0.261M) NaOH, 2.5% (0.677M) $NaBH_4$. It is concluded that most of the hydrogen was generated from the reaction of aluminum with sodium hydroxide. The dissolution of $NaBH_4$ in alkaline solutions increases the hydrogen generation rate of aluminum in the presence of EDTA. However, it is important to differentiate the hydrogen generation from hydrolysis of $NaBH_4$ and the hydrogen from the reaction of aluminum and NaOH.

Although the catalytic activity of aluminum alloy for hydrolysis of sodium borohydride is not fully investigated, the use of aluminum with alkaline solutions as a hydrogen source is expected to be a promising hydrogen source. Additional researches in this area are expected in the future.

Chapter 5

RECOMMENDATIONS

Cobalt on nanostructured PPX films / Cobalt metallic powder

(1) The variations in hydrogen generation rates of nanostructured Co-PPX films are needed to be investigated further more. Palladium was used in the process of PPX-film metallization. Surface composition analysis though EDAX was performed to assure that of palladium is not present and it is not exposed through surface cracks of the Co-PPX films which might form when the Co-PPX films are used as catalyst in contact with the $NaBH_4$ solutions. Surface analysis of the Co-PPX films by EDAX after contacting solutions may reveal the exposure of palladium and this is recommended for future work. However, it is strongly recommended in future works to always perform surface analysis by EDAX to assure that only the deposited metals become in contact with the solutions.

(2) Certain degree of inhomogeneities on the films used as catalyst in the experiments, those inhomogeneities were primary due to the lack of control on the nano-polymeric structures. The development of high conformal polymerization of nanostructured PPX films may also improve the reproducibility of the hydrogen generation of Co-PPX catalyst and this is also recommended for future work.

(3) In this research work, only cobalt PPX films were explored. However, is has been well identified in the literature that nanoscale binary metals (for example, Co-B) and other metals are also good catalyst. Therefore, deposition of those metals on the

nanostructured PPX films and their performance on hydrogen generation should be explored.

(4) As an effort to reduce the cost of Co-PPX or metal-PPX films, an investigation the use of inexpensive metals instead of Pd in metallization process is also recommended.

(5) In evaluating the catalytic activity of different catalysts used to produce hydrogen (or any other gas), is well accepted among the experimental scientific community that part of the catalyst area become blocked (from the electrolyte contact) by the gas bubbles being evolved at the catalyst surface. A good mathematical treatment that can e used to calculate or estimate the changes of catalyst surface with time and due to the gas evolution attached at the catalyst surface. In order to give an accurate number of milliliters of hydrogen evolved per unit of area of the catalyst this problem has to be addressed. In this work, the effective catalyst surface reduction, which is dependent on the blockage occurred by the gas bubble, was not considered. The formations of hydrogen bubbles on the Co-PPX films surface were observed during the hydrolysis of $NaBH_4$. They probably block the access of reactants and caused the reduction of hydrogen generation and unreliable results. Therefore, it is needed to develop effective method to prevent the bubble formation on the Co-PPX catalyst surface.

(6) On the same token, different authors use different ways to calculate the number of catalyst molecules in contact with the electrolyte, and calculate the gas evolution on milliliters of gas by units of weigh of catalyst. This problem becomes more difficult to calculate when the shape of the catalyst is spherical or other than flat. The ways of making those calculations may be the difference between poor and good findings

in a given paper. There is not in the literature (to our knowledge) a accepted way to calculate the weight of catalyst. By this important reason we did not present our result on liters/gram of catalyst. It is very important in future works that his problem is seriously addressed and solved and a general well established method to use the gas volume/weight of catalyst to be used by the catalyst scientific community. There is not a standard method to define the weight of the catalysts. Only the atoms on the surface of catalysts are actually in contact with the solutions. Therefore, the development of reasonable and logic weight calculation of catalysts is recommended.

(7) Nanostructures present a challenge in the calculation of the natural potential that the metals or metal alloys adopt when in contact with an electrolyte. The reason is that ionic local concentration of the electrolyte in contact with the nanostructure can modify the open circuit potential or mixed potential. Potential contribution from nanostructure “peaks” and “valleys” at the surface can become important. It is essential to understand the effect that nanostructures have over catalysts. Thus, a systematic testing of the effect of catalyst polarization on hydrogen generation in alkaline stabilized $NaBH_4$ solutions is recommended for future research.

(8) A very important variable not explored in this research is the effect of temperature on the catalysis of $NaBH_4$ solutions.

(9) The addition of EDTA and deaeration of the solutions probably change the nature of the oxide film. As mentioned in Chapter Three, the exact structure of oxide film and its compositions on the surface of cobalt catalyst in both naturally aerated and deaerated solutions should be investigated in more detail. The recommendation is to use techniques such as x-ray photoelectron spectroscopy for insightful understanding of the

cobalt catalyst in this application for the characterization of oxide films on cobalt in alkaline stabilized $NaBH_4$.

Aluminum alloy

(1) The effect of NaOH concentrations was investigated. For the enhanced hydrogen generation rate, it is recommended to evaluate both the effect of $NaBH_4$ concentration as well for the hydrogen generation rate of aluminum.

(2) As mentioned in Chapter Four, it is important to differentiate the hydrogen generation from hydrolysis of $NaBH_4$ and the hydrogen from the reaction of aluminum and NaOH. Therefore, it is recommended to use of deuterium either as solvent (D_2O) or as BD_4^-. The evolved hydrogen and deuterium can be analyzed by mass spectroscopy. By doing so, the exact amount hydrogen from hydrolysis of $NaBH_4$ and reaction of aluminum in alkaline solutions can be measured.

(3) It is recommended to study of aluminum alloys as catalysts for hydrogen evolution. Also, the influence of aluminum dissolution in the electrolyte and change of electrolyte compositions over time needs to be explored.

Bibliography

1. Wee, J.-H., K.-Y. Lee, and S.H. Kim, *Sodium borohydride as the hydrogen supplier for proton exchange membrane fuel cell systems.* Fuel Processing Technology, 2006. **87**(9): p. 811-819.

2. Schlesinger, H.I.B., Herbert C.; Hoekstra, Henry R.; Rapp, Louis R., *Reactions of diborane with alkali metal hydrides and their addition compounds. New syntheses of borohydrides. Sodium and potassium borohydrides.* Journal of the American Chemical Society, 1953. **75**: p. 199-206.

3. Kreevoy, M.M.J., R. W., *The rate of decomposition of sodium borohydride in basic aqueous solutions.* Ventron Alembic, 1979. **15**: p. 2-3.

4. Richardson, B.S., et al., *Sodium borohydride based hybrid power system.* Journal of Power Sources, 2005. **145**(1): p. 21-29.

5. Park, E.H., et al., *Recycling of sodium metaborate to borax.* International Journal of Hydrogen Energy, 2007. **32**(14): p. 2982-2987.

6. Kojima, Y. and T. Haga, *Recycling process of sodium metaborate to sodium borohydride.* International Journal of Hydrogen Energy, 2003. **28**(9): p. 989-993.

7. Patel, N., et al., *Pulsed-laser deposition of nanostructured Pd/C thin films: A new entry into metal-supported catalysts for hydrogen producing reactions.* Applied Surface Science, 2007. **254**(4): p. 1307-1311.

8. Krishnan, P., K.-L. Hsueh, and S.-D. Yim, *Catalysts for the hydrolysis of aqueous borohydride solutions to produce hydrogen for PEM fuel cells.* Applied Catalysis B: Environmental, 2007. **77**(1-2): p. 206-214.

9. Kim, J.-H., et al., *Production of hydrogen from sodium borohydride in alkaline solution: development of catalyst with high performance.* International Journal of Hydrogen Energy, 2004. **29**(3): p. 263-267.

10. Kim, J.-H., et al., *Study on degradation of filamentary Ni catalyst on hydrolysis of sodium borohydride.* Journal of Alloys and Compounds, 2004. **379**(1-2): p. 222-227.

11. Wu, C., et al., *Cobalt boride catalysts for hydrogen generation from alkaline NaBH4 solution.* Materials Letters, 2005. **59**(14-15): p. 1748-1751.

12. Kojima, Y., et al., *Hydrogen generation using sodium borohydride solution and metal catalyst coated on metal oxide.* International Journal of Hydrogen Energy, 2002. **27**(10): p. 1029-1034.

13. Amendola, S.C., et al., *A safe, portable, hydrogen gas generator using aqueous borohydride solution and Ru catalyst.* International Journal of Hydrogen Energy, 2000. **25**(10): p. 969-975.

14. Lee, J., et al., *A structured Co-B catalyst for hydrogen extraction from NaBH4 solution.* Catalysis Today, 2007. **120**(3-4): p. 305-310.

15. Cho, K.W. and H.S. Kwon, *Effects of electrodeposited Co and Co-P catalysts on the hydrogen generation properties from hydrolysis of alkaline sodium borohydride solution.* Catalysis Today, 2007. **120**(3-4): p. 298-304.

16. Ingersoll, J.C., et al., *Catalytic hydrolysis of sodium borohydride by a novel nickel-cobalt-boride catalyst.* Journal of Power Sources, 2007. **173**(1): p. 450-457.

17. Pena-Alonso, R., et al., *A picoscale catalyst for hydrogen generation from NaBH4 for fuel cells.* Journal of Power Sources, 2007. **165**(1): p. 315-323.

18. M. C. Demirel, M.C., A. Singh, W. J. Dressick, *Noncovalent Deposition of Nanoporous Ni Membranes on Spatially Organized Poly(p-xylylene) Film Templates.* Advanced Materials, 2007. **19**(24): p. 4495-4499.

19. Demirel, M.C., et al., *Spatially Organized Free-Standing Poly(p-xylylene) Nanowires Fabricated by Vapor Deposition.* Langmuir, 2007. **23**(11): p. 5861-5863.

20. M. Cetinkaya, N.M.a.M.C.D., J. Polym. Sci. B: Polym. Phys. 46 (2007), pp. 640–648.

21. A. Cetinkaya, S.B.a.M.C.D., Polymer 48 (14) (2007), pp. 4130–4134.

22. Malvadkar, N., et al., *Catalytic activity of cobalt deposited on nanostructured poly(p-xylylene) films.* Journal of Power Sources, 2008. **182**(1): p. 323-328.

23. Brown, H.C. and C.A. Brown, *New, Highly Active Metal Catalysts for the Hydrolysis of Borohydride.* J. Am. Chem. Soc., 1962. **84**(8): p. 1493-1494.

24. Zhang, L., K. Lee, and J. Zhang, *Effect of synthetic reducing agents on morphology and ORR activity of carbon-supported nano-Pd-Co alloy electrocatalysts.* Electrochimica Acta, 2007. **52**(28): p. 7964-7971.

25. Amendola, S.C., et al., *An ultrasafe hydrogen generator: aqueous, alkaline borohydride solutions and Ru catalyst.* Journal of Power Sources, 2000. **85**(2): p. 186-189.

26. Wu, C., H.M. Zhang, and B.L. Yi, *Hydrogen generation from catalytic hydrolysis of sodium borohydride for proton exchange membrane fuel cells.* Catalysis Today, 2004. **93-95**: p. 477-483.

27. Wu, C., et al., *Cobalt boride catalysts for hydrogen generation from alkaline NaBH4 solution.* Materials Letters, 2005. **59**(14-15): p. 1748-1751.

28. Krishnan, P., et al., *PtRu-LiCoO2 - an efficient catalyst for hydrogen generation from sodium borohydride solutions.* Journal of Power Sources, 2005. **143**(1-2): p. 17-23.

29. Lee, J., et al., *A structured Co-B catalyst for hydrogen extraction from NaBH4 solution.* Catalysis Today, 2007. **120**(3-4): p. 305-310.

30. Pourbaix , M., *Atlas of Electrochemical Equilibria in Aqueous Solutions*. 1966, New York: Pergamon.

31. Lieth, R.M.A., *Preparation and Crystal Growth of Materials with Layered Structures*. 1977: Springer.

32. Badawy, W.A., F.M. Al-Kharafi, and J.R. Al-Ajmi, *Electrochemical behaviour of cobalt in aqueous solutions of different pH.* Journal of Applied Electrochemistry, 2000. **30**(6): p. 693-704.

33. Ismail, K.M. and W.A. Badawy, *Electrochemical and XPS investigations of cobalt in KOH solutions.* Journal of Applied Electrochemistry, 2000. **30**(11): p. 1303-1311.

34. Belitskus, D., *Reaction of Aluminum with Sodium Hydroxide Solution as a Source of Hydrogen.* Journal of The Electrochemical Society, 1970. **117**(8): p. 1097-1099.

35. Soler, L., et al., *Synergistic hydrogen generation from aluminum, aluminum alloys and sodium borohydride in aqueous solutions.* International Journal of Hydrogen Energy, 2007. **32**(18): p. 4702-4710.

36. Macdonald, D.D., S. Real, and M. Urquidi-Macdonald, *Evaluation of Alloy Anodes for Aluminum-Air Batteries.* Journal of The Electrochemical Society, 1988. **135**(10): p. 2397-2409.

Appendix A

Achievement

Publication

Malvadkar, N., Park, S. Urquidi-MacDonald, M., Wang, H. and Demirel, M.C., *Catalytic activity of cobalt deposited on nanostructured poly(p-xylylene) films.*, Journal of Power Sources, 2008. **182**(1): p. 323-328.

Posters

(1) *Hydrogen Release Application of Cobalt Membrane Deposited on Nanostructured Polymer Film Template*, Annual Graduate Exhibition, Graduate School, 2008.

(2) *Cobalt on Nanostructured Polymer Film Template as a Catalyst for Hydrogen Generation Applications*, Annual Poster Competition, Department of Materials Science and Engineering, 2008.